7-1-2013

Development of CD19 binding reagents for targeted nanoparticles

Jason Hugh Rogers

Jason H. Rogers
Candidate

Pathology
Department

This thesis is approved, and it is acceptable in quality and form for publication:

Approved by the Dissertation Committee:

Walker Wharton, Ph.D., Chairperson

David Peabody, Ph.D.

Helen Hathaway, Ph.D.

i

**DEVELOPMENT OF CD19 BINDING REAGENTS FOR
TARGETED NANOPARTICLES**

BY

JASON H. ROGERS

**B.S., BIOLOGY
NEW MEXICO STATE UNIVERSITY, 2004**

THESIS

Submitted in Partial Fulfillment of the
Requirements for the Degree of

Master of Science

Biomedical Sciences

The University of New Mexico
Albuquerque, New Mexico

July 2013

DEDICATION

For my parents, Rev. Hugh, & Janice Rogers,

    My endless and unfailing support.

For Mrs. Cooper, my fourth grade teacher,

    *Who taught me how to be a student in **all** subjects, and how to work,*

For Mrs. Halbig, my high school biology teacher,

    Who gave her very soul, imparting her passion for science and knowledge,

      The only teachers I ever needed.

ACKNOWLEDGEMENTS

DEVELOPMENT OF CD19 BINDING REAGENTS FOR TARGETED NANOPARTICLES

By

Jason H. Rogers

B.S., Biology, New Mexico State University, 2004

M.S., Biomedical Sciences, University of New Mexico, 2013

ABSTRACT

B-cell malignancies like Acute Lymphoblastic Leukemia (B-ALL), which often have high numbers of malignant cells in circulation in the blood would be an excellent model system for the early preclinical development and testing of targeted small particle therapeutics. We selected the transmembrane protein CD19 (Cluster of Differentiation 19) as one potential promising target due to its remarkably common over-expression on nearly every case of B-ALL, and on many other types of leukemias and lymphomas with varying frequency. We attempted to create a panel of appropriate CD19-specific targeting reagents for attachment to the surface of perhaps many different small particle platforms currently in development worldwide. We first utilized an M13 bacteriophage random peptide display library to attempt to isolate a short CD19-binding peptide using both a cell-based and a purified protein-based strategy. Despite multiple attempts, neither of these approaches yielded the discovery of such a peptide. We have, however, in process, developed novel phage purification procedures that we demonstrate are particularly important when validating the binding of clones recovered from the library using two cell-based assays; these consist of a simple flow cytometry method and a complex, but

higher throughput, assay done in 96-well plates that can measure phage binding to cells with a qPCR approach. As a second strategy for making targeting reagents, we expressed and refolded large quantities of two known anti-CD19 Single-chain Fv fragments from cytoplasmic inclusion bodies in *E. coli.* We here demonstrate that one of them, HD37 (originally isolated from a mouse hybridoma cell line as an IgG1 subtype) could be refolded into a somewhat active form by using a previously published procedure. A second antibody fragment, FMC 63 (also originally from mouse hybridoma, an IgG2 subtype) did not refold properly by this procedure and work is ongoing to find a suitable refolding strategy for this antibody in particular. Thus, we proffer the recombinant HD37 antibody fragment as the simplest strategy for the production of large quantities of CD19-targeting reagent suitable for attachment to small particle therapeutics, as we find that CD19 is particularly challenging to use as a target for phage display technologies in the cell context.

TABLE OF CONTENTS

viii

LIST OF FIGURES

INTRODUCTION

Chemotherapeutics are changing. An increasing number of nano-sized particle delivery systems are being developed that show potential as novel drug carrier therapeutics; these include liposomes, micelles, particles with a gold or silica core and some polymer coating, and many others (Davis et al., 2008). A large proportion of these platforms are developed with solid tumors in mind, and mainly propose to be efficacious by means of the Enhanced Permeability and Retention (EPR) phenomenon (Matsumura and Maeda, 1986), wherein the grossly malformed tumor vasculature, often described as leaky, allows for 'targeting' by a simple buildup of particles (10-100nm size range) and subsequent release of drug in the tumor tissue.

Of particular interest to our group are targeted particles for use against leukemia, where the EPR effect is limited and instead, a better system would be long-circulating particles that can interact specifically with leukemia cells and not the rest of the cells in the blood. While the targeting of the bone marrow is also an important question, this will probably depend more on the particular nanoparticle characteristics, and less on the targeting ligands attached to the surface. Thus, the emphasis of this thesis was to develop targeting ligands that could potentially be used with many different nanoparticle platforms. We focused on a very common leukemia/lymphoma target, CD19, that is highly expressed in almost all cases of Acute Lymphoblastic Leukemia, or ALL (Lee-Sherick et al., 2010), and we took two basic approaches: 1.) Discovery of novel, short peptides that bind specifically to CD19; 2.) Purification of large quantities of known

1

single-chain Fv antibody fragments against CD19. Short peptides and small but active antibody fragments may help maintain minimal immunogenicity (Reilly et al., 1995) of the particle, if evidence about these proteins used in isolation translates when they are attached to a particle surface. A comprehensive understanding of the important contributing factors to the ultimately enormous variety of potential immune responses to complicated nanoparticle platforms is not well understood, and must often be analyzed on a case-by-case basis, or even batch-by-batch. The initial hurdle to overcome is to successfully develop targeting reagents that can then be attached to nanoparticle platforms and tested *in vitro* to see if they confer specificity of the particle in delivering a cargo exclusively or preferentially to CD19-positive cells, which includes most ALL cases.

Acute Lymphoblastic Leukemia

Over 25% of all cancer deaths in children result from B-cell precursor ALL. Changes in chemotherapy regimens for pediatric ALL and markedly improved risk classification have increased five-year survival rates from less than 10% to near 80% over the last fifty years (Pui, 2010). Despite these encouraging advances, critical improvements are needed based on several important facts:

1.) 6.5-17 % of pediatric patients do not survive ALL, depending on the clinical trials and protocols they were treated under (Pui, 2010). Previous research in our laboratory has been heavily focused on this group of patients and we have utilized gene

2

expression analysis to identify a subset of patients that have very poor five-year event-free survival (EFS) rates (Harvey et al., 2010). Strikingly, we have also found that Hispanic and Native American children are more than twice as likely to fall under this high-risk category and have been found to have a consistently poorer prognosis (Yang et al., 2011).

2.) About 2/3 of patients who survive their original disease and chemotherapy treatments suffer from a vast array of side effects and complications including reproductive sterility, cardiovascular problems, neurological deficits, stunted growth, and many others, sometimes even including secondary neoplasms. About 25% of these therapy-related sequelae are considered severe (Pui, 2010).

3.) Steady improvements in outcome over the years have resulted mostly from improved risk-stratification (by cytogenetic tests and immunophenotyping) and painstaking timing/dose optimization in large clinical trials. Few first-line drug treatments have been developed in the past 30 years. Additionally, outcomes for adults over the age of 18 with Acute Lymphoblastic Leukemia remain extremely poor and virtually unchanged during this same period (Lee-Sherick et al., 2010).

Clearly, novel therapeutic approaches are needed to minimize side-effects and provide a more tolerable option for patients who require high-toxicity dosing to achieve remission and especially for those resistant to all treatments. Targeted small particle therapies are one important approach in this consideration.

3

CD19 as a therapeutic target

A common cell-surface receptor found in almost all B-cell lymphomas and leukemias is CD19, or Cluster of Differentiation 19 (reviewed in Lee-Sherick et al., 2010). CD19 augments signaling through interaction with the B-cell antigen receptor (BCR) and is vital for maintenance of survival/proliferation programs in normal and cancerous B-cells (Pezzutto et al., 1987). Expression of this protein under normal B-cell development is limited to mid-B-cell stages; and, it is not expressed on any type of early or late hematopoietic stem cell or plasma cells-- mature, antibody secreting B-cells (Pedersen et al., 2002; Uckun et al., 1988). Normal B-cells could potentially be depleted by this and other developing CD19-targeted therapies, but they should repopulate over time from hematopoeitic stem cells. CD19 is also measurably expressed on follicular dendritic cells (FDC; mesenchymal cells found in lymphoid follicles), though the expression level is 10- to 100-fold less relative to most leukemia cells. Due to this markedly different level of expression, we expect to be able to preferentially target neoplastic B-cells. However, this potential off-target effect in FDCs may prove beneficial, as evidence shows they secrete a protective cytokine, CD154, to perpetuate survival of drug-resistant B-cell Chronic Lymphoblastic Leukemia (Pedersen et al., 2002).

Other therapies using CD19-targeted liposomes and toxin-conjugated monoclonal antibodies (mAb) are also currently in development. CD19 and mAbs bound to it are rapidly internalized in many leukemia cell lines (Ingle et al., 2008), though a very recent

4

claim of the discovery of a CD19 ligand (CD19-L, expressed on multiple lymphoid cell subtypes, including T-cells) shows simple binding of this ligand to the receptor (and potentially CD19-L mimics) specifically causes apoptosis (Uckun et al., 2011). Corroboration of this finding has not yet been published, however.

Clinical Use of Recombinant Antibodies

About 20 monoclonal antibodies have been approved by the FDA are in use clinically in the United States, and many others are in various stages of clinical trials (Reichert and Dewitz, 2006). These antibodies vary from mouse, chimeric (human and mouse), humanized (mouse Fv region with human Fc amino acids) and fully human, and there is a general trend that more humanized or human antibodies have lower rates of side-effects, though many side-effects depend very much on the target. A large proportion of these recognize targets directly available by intravenous injection that are present on blood cells, such as B- and T-cells, and often aid in the treatment of autoimmune disorders and blood cancers (Hansel et al., 2010). In a fraction of patients, an antibody response is sometimes mounted against the therapeutic antibody, and some reports even associate more favorable outcome in B-cell cancers with the production of Human Anti-Mouse Antibodies (Azinovic et al., 2006), though this may simply reflect undetectable differences in the functionality of what remains of the hematopoietic system. As a whole antibodies are a relatively safer therapy than many traditional small molecule drugs, and indeed antibodies are four times more likely to proceed through clinical trials to FDA approval that equivalently staged drugs (Reichert et al., 2005).

5

Occasionally, the side effects can be severe, as in the case of an anti-CD28 monoclonal antibody (TGN1412) that caused life-threatening cytokine storm from T-cell over-activation in six healthy volunteers after a single dose (Suntharalingam et al., 2006).

Full-sized monoclonal antibodies have been successfully conjugated to nano-sized particles and shown to target specific receptors *in vivo* (Hathaway et al., 2011). Single-chain Fv (scFv) fragments, while lacking the stimulatory Fc region associated with the efficacy of the opsonization of cells intended for removal by antibody therapies, may be the best option when considering attachment to particles. They are the least immunogenic portion of the antibody and they can be cloned and readily expressed in bacterial systems, though their refolding from cytoplasmic fractions remains challenging. We used two different mouse anti-human CD19 scFvs, HD37 and FMC63.

Phage Display libraries

While free peptides are extremely short-lived in the blood stream, they may have a longer half-life when attached to a particle system. They would be immensely less expensive to produce than recombinant antibodies, and there is a well-known system that has been used to identify peptides that interact with specific cell surface receptors.

Filamentous or fd phage are a type of virus that are highly infectious to *E. coli.* As suggested by their name, they have a very elongated filamentous structure that is about 900nm in length but with only an 8nm diameter. Of particular interest are the five copies

6

of the PIII protein which protrude quite dramatically from one end of each phage particle (Pratt et al., 1969) and are responsible for the initial attachment of the phage to the F-pillus on F+ strains of *E. coli* and other gram-negative bacteria (Gray et al., 1981), which ultimately leads to infection of a bacterium.

Extending on these studies, a seminal publication by George Smith (Smith, 1985) showed that genetically fusing fragments of the EcoRI endonuclease to the PIII protein allowed for specific capture of the phage via an anti-EcoRI antibody, and that these perturbations in the phage genome only mildly affected its infectivity and competition with wild-type phage. He further proposed that entire libraries could easily be created containing short peptides or antibody fragments fused to the PIII protein that could be used for discovery of ligands or vaccine production by creating an antibody response against the displayed epitope after injection of whole phage particle into animals.

Since that initial discovery, his laboratory has created a vital resource of phage handing protocols for other researchers. Many of the protocols developed in this work are derived from this resource, found online at:
http://www.biosci.missouri.edu/smithgp/PhageDisplayWebsite/PhageDisplayWebsiteIndex.html.

Additionally, Smith's laboratory has created a large number of different phage display libraries with both 6- and 15-amino acid inserts for various purposes, most of which are still available free of charge from his research group, since they have never

7

patented the technology and instead were more motivated to make an infinitely useful research tool available to the entire scientific community. Since that time, New England Biolabs has commercialized a variant of Smith's libraries, both a 7-amino acid and 12-amino acid library. We used both the 7-and 12-amino acid libraries from NEB in our studies, the major difference being that these libraries contain a LacZ cassette instead of a Kanamycin resistance cassette, which allows for blue white color selection and differentiation of library vs. wild type phage plaques.

Caveats to phage display: Target unrelated outgrowths

Phage display libraries are imperfect screening tools and caution must be used to avoid making erroneous conclusions about the peptides that come about from the sequences at the end of several rounds of phage display. A number of phage clones, primarily from the NEB PhD 7-mer library, have been identified with different properties that provide a target-unrelated selection advantage. One phage in particular with the peptide insert HAIYPRH was isolated independently by several groups and claimed to have specific binding activity for a variety of seemingly unrelated targets, including the following: antibody epitopes against the cucumber mosaic virus Fny-CMV (He et al., 1998); human transferrin receptor (Lee et al., 2001); chromatin HMGB1 protein (Dintilhac and Bernués, 2002); A549 adenocarcinomic human alveolar basal epithelial cells (Rahim et al., 2003); and human umbilical vein endothelial cells (Maruta et al., 2003).

8

Brammer et al., (2008) also isolated this same phage that came through their screens while attempting to identify peptides that can bind to immobilized Zn^{2+}. A simple literature search of the recovered peptide sequences revealed this peculiarity to them and it seemed unlikely that the peptide HAIYPRH actually possessed the entire gamut of, purportedly, specific yet diverse binding activities when the above work was considered as a group. They performed a careful analysis and complete genomic sequencing of this phage (6407 bases of ssDNA (Smith and Petrenko, 1997)), and, when compared to the parent vector from which the library was derived, they discovered a single point mutation in the Shine-Dalgarno16s-ribosomal RNA complementarity binding region for the gIIp gene that markedly increased the growth rate of this phage over whole library or an insert-less clone lacking a random peptide displayed on pIII (Brammer et al., 2008).

Problems also arise with target-unrelated phage that can bind to other components of the display system than the protein or cell surface receptor of interest; for example, peptides displayed on clones isolated from library screens have been shown to interact with polystyrene plates (Adey et al., 1995) and streptavidin (which is commonly used conjugated to agarose beads to pull down biotinylated target proteins theoretically bound to phage) by a family of different peptides containing an HPQ motif (Weber et al., 1992), which is not affected by integration into a circularized motif used in some phage display libraries (Giebel et al., 1995). Phage with the sequence FHENWPS have also been shown to bind to bovine serum albumin (Brammer et al., 2008), though it has been argued this is simply another polystyrene binder (Vodnik et al., 2011).

9

Target-unrelated phage are well-documented, and some are well-characterized, though the appreciation of their commonness and their propensity to cause research groups not well-practiced in phage display technology to make incorrect claims about the binding affinity is clearly underappreciated. This calls for a need to optimize or create new screening procedures that could be used to test phage clones rapidly in a cell-based system. This also makes it extremely important to validate specific binding of phage clones to the target by at least two completely unrelated methods.

Thus, with these two different strategies, discovery of short CD19-interacting peptides and production of known scFv recombinant antibody fragments in bacteria, we set out to develop our own stocks of targeting reagents against CD19.

Cell lines

All human and mouse cell lines were cultured in aseptic conditions at 37°C in a humidified chamber supplemented with 5% CO_2. All were purchased from American Type Culture Collection (ATCC) except where otherwise noted. Molt4, Jurkat, Reh, Nalm6 and MHH-CALL4 cell lines and their derivatives were cultured in RPMI supplemented with 10% v/v Fetal Bovine Serum (Atlanta Biologicals) L-Glutamine (2.05mM), 100 units of penicillin and 100 μg of streptomycin per mL (Life Technologies). Ba/F3 cells were cultured in the above media with the addition of 10% WEHI-3B conditioned medium as a source of Interluekin-3 (Lee et al., 1982). 293-FT cells were cultured in DMEM supplemented with 10% v/v Fetal Bovine Serum (Atlanta Biologicals), L-Glutamine (2.05mM), 100 units of penicillin and 100 μg of streptomycin per mL (Life Technologies).

Cell counting

For flow cytometry and panning viability experiments, cell viability was measured using a VI-CELL automated cell counter (Becton Dickenson) that measures viability by trypan blue exclusion.

11

Plasmids and cloning

The full length CD19 gene (plasmid from OpenBiosystems) was PCR amplified and subcloned into the pLNCX2 retroviral plasmid (Clontech) into the XhoI-NotI restriction sites using standard molecular biology techniques. The sequence was verified using Sanger Sequencing services from Eurofins MWG Operon. Plasmids were propagated by transformation of electrocompetent DH5-alpha *E. coli* and purified with a standard endotoxin free maxi prep kit (Omega Bioscience).

Retrovirus

293-FT cells were grown to 50% confluence in 100mm tissue culture dishes and transfected by calcium phosphate precipitation with the pLNCX2 parent vector or pLNCX2-CD19. Each plate was co-transfected with the pCL-Ampho retroviral helper plasmid. Retrovirus was recovered from the supernatant 48-72 hours later and concentrated with Centricon Plus-80 centrifugal filters (Amicon) with a 10,000 Dalton MW cut-off. 500μL of 10X concentrated retroviral supernatant was added directly to 1 million cells, either Molt4 or Jurkat, and seeded into six-well plates. Polybrene (Santa Cruz Biotech) was added to the infection at a concentration of 5μg/mL. Spinfection was performed as previously described (Ho et al., 1993) subjecting the virally infected cell cultures to centrifugation at room temperature for 90 minutes at 2000 RPM in their six well culture dishes. 48 hours after retroviral transduction, Geneticin (CellGro) was added to the cultures at 600 μg/mL for Molt4 and 1000 μg/mL for Jurkat cells. Selection was

12

continued for 14-21 days until all of the cells in an untransduced control sample died. After selection, cells were maintained in a maintenance Geneticin dose of 100 μg/mL.

RNA isolation and detection of CD19 mRNA by qRT-PCR

1×10^6 cells were collected and centrifuged at 1500 RPM for five minutes at 4°C. The supernatant was aspirated and the cell pellet was immediately resuspended in Trizol (Life Technologies). RNA was isolated according to the manufacturer's instructions. RNA concentration was determined by a NanoDrop spectrophotometer and 100ng was used for the reverse transcription reaction, using the Superscript III RT kit (Life Technologies), priming the poly-A-mRNA with oligo-dT. 2.5μL of the reverse transcription reaction was used as input for quantitative PCR detection with Taqman primer sets designed to recognize CD19 and 2X Taqman Universal PCR Mastermix (Life Technologies). The reactions were run on an ABI Prism quantitative PCR machine and the C(t) values were recorded and relative values were analyzed by the $2^{-\Delta\Delta C(t)}$ method.

Flow cytometry for the detection of CD19 overexpression

0.5 million cells were washed in PBS/0.5%BSA and resuspended in 100μL PBS/0.5%BSA. 20 μL of anti-CD19 mouse monoclonal antibody (phycoethrin-conjugated, BD Biosciences) were added to each sample and incubated at 4°C for one hour. Cells were washed one final time in PBS and resuspended in 350 μL PBS for

13

detection by flow cytometry on a FACS Caliber. All cell sorting was carried out on a
MoFlo sorting apparatus from Becton Dickenson with expert technical assistance from
the UNM Cancer Center's Flow Cytometry Shared Resource.

Phage Display on live cells

Ph.D.™-12 and Ph.D.™-7 Phage Display Peptide Library Kits were purchased
from New England Biolabs. Detailed, step-by-step methods are provided in the Appendix
section.

Phage Display on purified protein

Recombinant human CD19 was purchased from Sino Biological. It was produced
in HEK-293 cells and runs as a broad smear and not a single band on SDS-PAGE,
potentially indicating that it contains a variety of glycosylation moieties, similar to
endogenous CD19 on normal B-cells. Its activity was verified by measurement of its
binding strength with a known interacting partner, CD81. The purity was approximately
95%.

Phage Display was carried out as described in the manufacturer's handbook with
minor modifications to a previously described protocol (Li et al., 2005). Three rounds
were carried out in total. In the first round, the phage were eluted once with 0.2M
Glycine, pH2.2. In the second round, the elution was repeated and the second elution was

14

used for the expansion culture for the input into Round 3. In the third round, a third elution was carried out and this elution was used directly for limited dilution plaque plating and sequencing of clones. The 12 amino acid library and the 7 amino acid library were panned in parallel by otherwise identical procedures.

Micropanning

Detailed step-by-step instructions are outlined in the Appendix. SYBR® Green PCR Master Mix was from Life Technologies. The primers used in the PCR reaction were the standard -96G III sequencing primer (5'-CCC TCA TAG TTA GCG TAA CG-3') and a second primer, Phage Plus4 (5'-GCC GAA ACT GTT GAA AGT TGT T-3') from the constant region upstream of the variable region that made a 109 bp amplicon.

Purification of phage stocks from a 50mL culture

Briefly, the manufacturer's instructions were followed for Day 1 and Day 2 (see Appendix), scaling up the volumes for a 50mL culture instead of 20mL used for the recommended procedure to amplify sub-libraries between rounds of selection. However, at the end of Day 2, a 10mL volume PEG/NaCl precipitation is carried out. The Day 3 Triton X-114 purification is modified from a protocol designed for removing lipopolysaccharide from protein samples (Aida and Pabst, 1990), adjusting the volumes where necessary and simply substituting phage particles instead of a crude or purified protein sample. The yield is approximately 1mL at ~1.0 x 10^{10} infectious particles/μL.

15

Other phage purification procedures

For data shown in Figure 9, phage stocks were all purified differently as follows. The number of 1:6 precipitations of 20%PEG-2.5M NaCl: Phage solution is shown and the precipitation was done overnight, except where noted 30 min. Samples mentioning Acetic Acid were processed as described in a protocol downloaded from Dr. George Smith's laboratory website by isoelectric precipitation in 0.1M Acetic Acid (Smith, 2006). For the Acetic Acid precipitation and also the samples using 1% Triton X-100, 1% CHAPS or 0.5% Tween, the extra step was before the final PEG/NaCl precipitation. The detergents were added after the previous PEG/NaCl precipitation each in different samples after resuspending the phage in 9mL of PBS. 1mL of a 10% stock solution of Triton X-100 or CHAPS, or a 5% stock solution for Tween were added and the samples were mixed vigorously and incubated on ice for 30 minutes before commencing with the final PEG/NaCl precipitation.

Phage binding to live cells: flow cytometry assay

Briefly, 0.5 million cells were alliquoted into standard flow cytometry tubes. For each phage clone to be tested, one tube of Molt4-pLNCX2 (control CD19-negative cells) and one tube of Molt4-pLNCX2-CD19 cells was used. Cells were washed 1X in 3mL PBS/0.5% Bovine Serum Albumin (BSA) at 4°C, for five minutes at 1500XRPM. After decanting the supernatant the cells were resuspended in 100μL PBS/BSA containing 10^{11} phage particles, purified by our newly described standard phage purification procedures

16

outlined in the Appendix. Cells mixed with phage were incubated for one hour at 4°C. Cells were washed again as above with 3mL PBS/BSA and the supernatants were decanted again. The cells were resuspended in 100μL PBS/BSA containing 5μL anti PVIII (phage coat protein), FITC-conjugated antibody from Fitzgerald, (Acton, MA; catalog #61R-M101aFT) and incubated for one hour at 4°C in the dark. Cells were washed again 3mL PBS as above and finally resuspended in 350 μL for analysis on a Becton Dickenson FACS Caliber.

Phage ssDNA sequencing and ssDNA preparation

Phage genomic ssDNA was purified by standard methods according to the manufacturer's instructions. This DNA was usually of low yield and poor quality so the original culture volume was doubled to 1mL and the final product was further purified by a PCR purification kit (Qiagen). The DNA recovered from this cleanup was then sequenced using Sanger sequencing services from Eurofins MWG Operon, with the standard sequencing primer 96 bases upstream of the random peptide insert, -96GIII. The sequence is 5' CCC TCA TAG TTA GCG TAA CG 3'. The resulting sequences were analyzed with Chromas DNA sequence analysis software and the amino acid insert sequences were determined.

17

Single-chain Fv antibody fragment purification

Both the HD37 scFv and the FMC63 scFv were subcloned into the pGEX-6-P1 vector (GE Life Sciences) at the N-terminal side of the *Schistosoma japonicum* Glutathione-S-Transferase gene as a fusion protein, connected by a cleavable linker specific to the ExScission protease (GE Life Sciences). The vector was transformed into an electro-competent BL-21 *E. coli* strain (Amersham) by electroporation and plating on LB agar plates containing 50μg/mL ampicillin sodium (Sigma-Aldrich). 500mL cultures of 2X YTA media supplemented with 50μg/mL ampicillin sodium were inoculated with a single colony and grown with vigorous shaking at 300 RPM at 37°C to an Absorbance of OD_{600}=0.6-0.8. At this culture density, IPTG (Sigma Aldrich) was added to the culture to 0.1 mM final concentration for induction of the expression of the fusion protein. The culture temperature was lowered to 22°C and shaking continued overnight for 18 hours. The cultures were subjected to centrifugation at 4°C for 30 min X 4000RPM and the bacterial pellet was resuspended well in 25mL Bacterial Protein Extraction Reagent supplemented with 1X Protease Inhibitor Cocktail (Pierce). The suspension was incubated on ice for 30 minutes and the centrifugation was repeated to pellet the insoluble matter which was found to contain the vast majority of the scFv-GST fusion protein. This lysed pellet containing inclusions bodies was further solubilized overnight with gentle agitation in a second 25 mL BPER lysis buffer aliquot supplemented with 2.5% CHAPS, 10% Sarkosyl, and 4% Triton X-100. The next day, the suspension was subjected to centrifugation for 30 minutes at 4000 RPM at 4°C and the supernatant was separated

18

from the remaining pellet which again contained the vast majority of the scFv-GST fusion protein.

This washed pellet containing largely inclusions bodies of scFv-GST was refolded into a functional form as previously described (Umetsu et al., 2003). Briefly, the inclusion body pellet was solubilized with gentle agitation overnight in 25mL 6M Guanidine HCl, 10mM beta-meracaptoethanol, 50mM Tris HCl (pH8.0), 200mM NaCl, 2mM EDTA (pH8.0). The following day the solution was again subjected to centrifugation for 30 minutes at 4000 RPM at 4°C and the concentration of protein in the supernatant was measured by Bradford Assay and diluted to 7.5μM in the same buffer, which was typically about a 1:25 dilution. Approximately 50% of the scFv-GST in the sample (by weight) could be solubilized by this method. The denatured protein was then injected into a 30mL dialysis cassette with a 10,000 Dalton molecular weight cutoff and dialyzed overnight at 4°C for each of the remaining steps, excluding the beta-mercaptoethanol and reducing the Guanidine HCl concentration from 6M, 3M, 2M, 1M, 0.5M, and 0M and finally into PBS. Importantly, at the 1M and 0.5M steps, L-arginine (400mM), and reduced glutathione (GSSG; 375μM) were added to the dialysis solution. The protein samples were then removed from the dialysis cassettes and stored at 4°C.

Flow cytometry for the detection of scFv

0.5 million cells were washed in PBS/0.5%BSA and resuspended in 100μL PBS/0.5%BSA. Varying amounts of scFv were added to the tube (1-100 μL) and the

19

samples were incubated at 4°C for one hour. Samples were washed again in PBS/BSA and resuspended as above, with the addition of 2µL Alexa-488-labeled anti-GST antibody (CellGro) and incubated again for one hour. Cells were washed one final time in PBS and resuspended in 350 µL PBS for detection by flow cytometry on a FACS Caliber (Becton Dickenson).

Engineering of CD19 overexpressing cell lines

In order to perform phage display on live cells with CD19 as the target, we needed pairs of cell lines that were, in principle, identical but for one having a complete lack of any CD19 expression and one that highly overexpressed CD19 on the cell surface, comparable to CD19 expression levels in leukemia cell lines. We selected for this purpose, the CD19-negative T-cell Acute Lymphoblastic Leukemia cell lines Molt-4 and Jurkat. The cells were transduced with the retroviral construct pLNCX2-CD19 or the parent vector pLNCX2. After two weeks of selection in G418, the overexpression at the RNA level was analyzed by qRT-PCR (Figure 1). CD19-positive controls shown are the B-ALL cell lines MHH-CALL4, Mutz5, Nalm6, and Reh. MV411 was used as a negative control along with the parental Molt-4 and Jurkat lines and their control vector-transduced counterparts. CD19 overexpression was quite significant and higher in both the Molt-4 pLNCX2-CD19 and Jurkat pLNCX2-CD19 than all of the positive control cell lines with the exception of MHH-CALL4.

21

Figure 1: CD19 expression by qRT-PCR
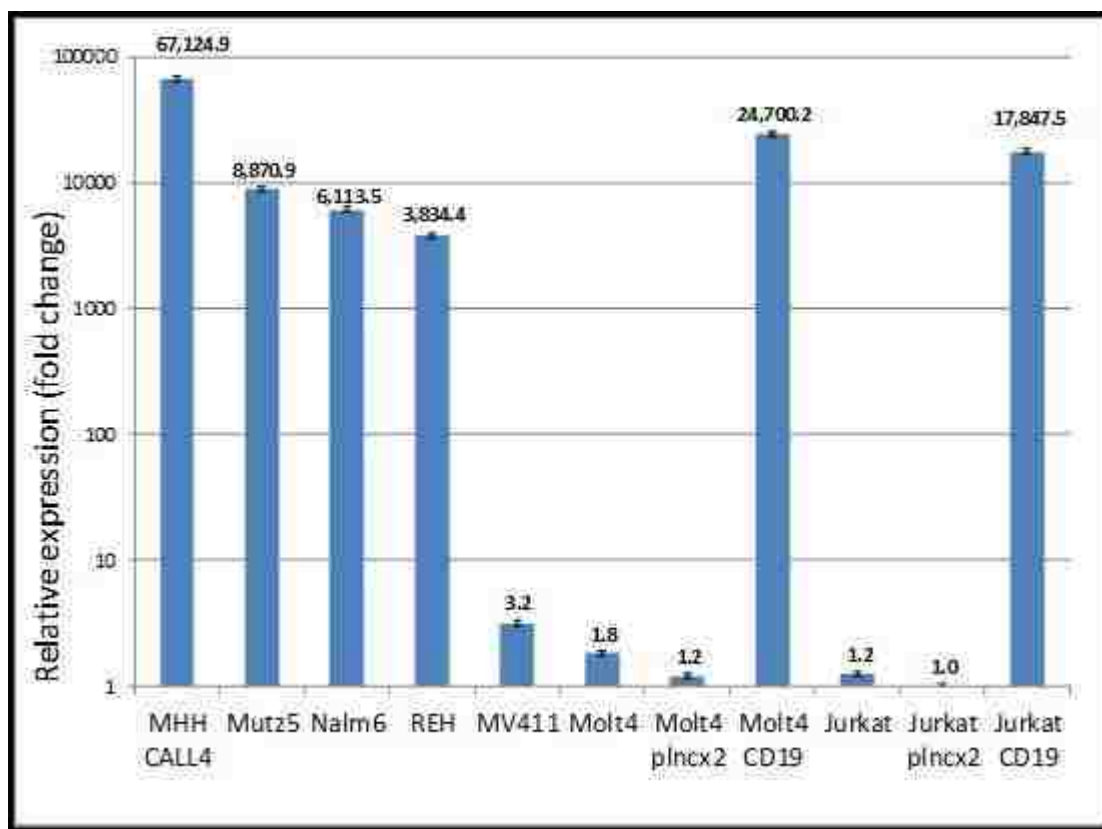
Naturally, we next needed to test that CD19 protein expression was comparatively high on the cell membrane by flow cytometry. We have observed quite frequently that some cell lines that are retrovirally transduced with membrane protein expression vectors may express high levels of the mRNA, but only express the protein in low amounts, or only intracellularly. We needed CD19 expression on the cell surface in order for it to be accessible to the phage particles during phage display selections. Figure 2A shows flow cytometry results measuring CD19 cell surface expression on two positive control cell lines, Mutz 5 and Nalm 6, and on the negative cell lines Molt-4 and Jurkat.

23

Figure 2A: Cell surface CD19 detection by flow cytometry: control cell lines
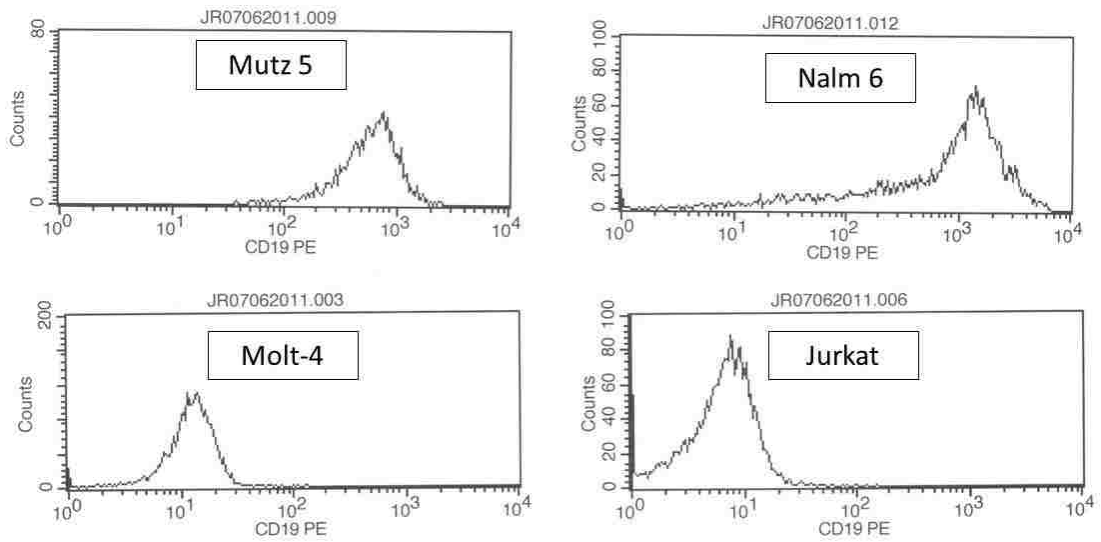
Figure 2B shows the retrovirally transduced and G418-selected CD19 overexpressing cell lines. Both the Molt-4 and Jurkat cell show high levels of CD19 expression on the cell surface, but the Molt-4-pLNCX2-CD19 cells have somewhat higher expression than their JurkatpLNCX2-CD19 counterpart cells. We did note, however, that there remained a subpopulation of each of these that was CD19-negative. This was a potential concern because of the increased possibility of recovering phage particles from these cells that would be bound to antigens other than CD19.

25

Figure 2B: Molt-4 and Jurkat CD19-overexpressing cell lines
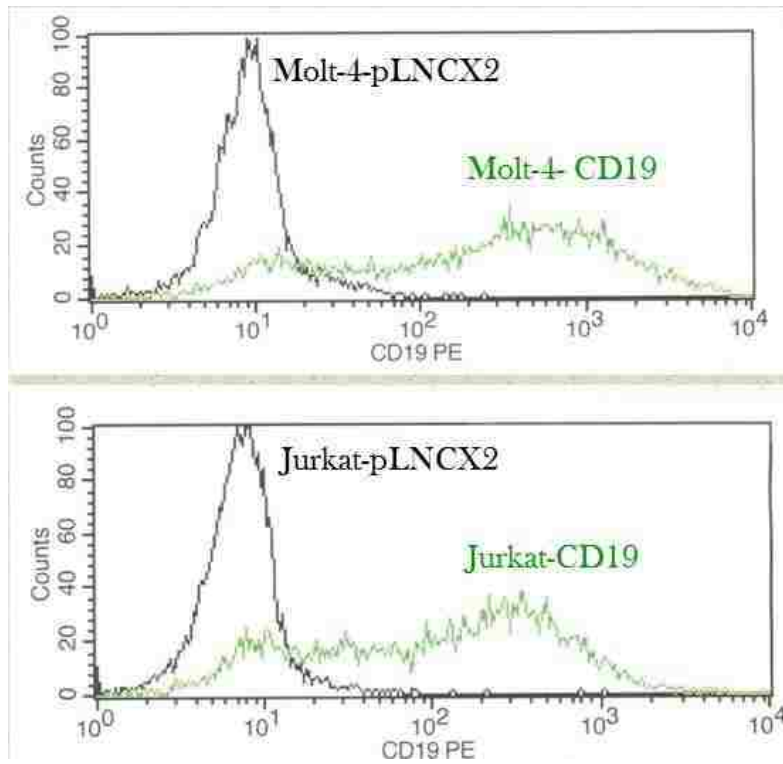
In order to achieve purer populations of CD19 overexpressors, we chose to sort the cells with the MoFlo sorting flow cytometer, as this method is faster and simpler and oftentimes sufficient for this purpose, as opposed to limiting dilutions and outgrowths of sets of clonal subpopulations. Figure 3 shows the sort gates set on CD19 expression of the Molt-4-pLNCX2-CD19 cells. We used these cells due to the fact that they exhibited increased CD19 expression compared to the Jurkat, and sorted the highest 10% and the next 25% into separate dishes and cultured the cells for two weeks.

Figure 3: Molt-4-pLNCX2-CD19 sorting gates
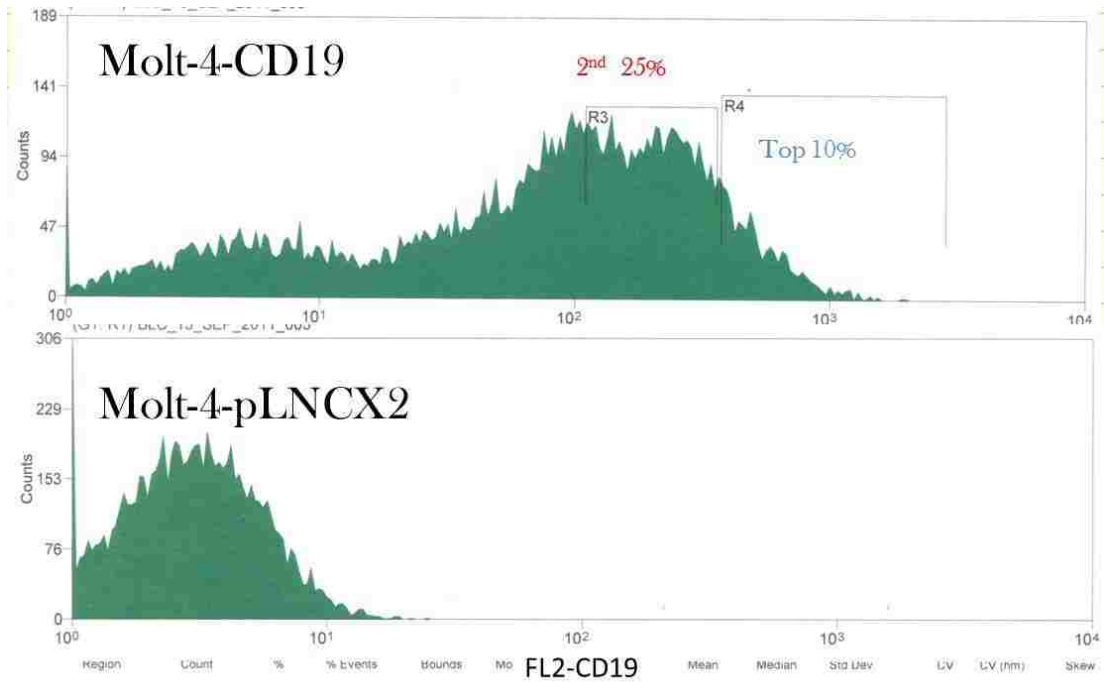
The cells were subjected to flow cytometry analysis again after the two week culture period, to ensure an expected increase in CD19 overexpression that was at least somewhat stable. Figure 4 shows this flow cytometry data. The 'Top 10%' samples showed the highest expression level of CD19, and these cells were used in all subsequent phage display experiments and also tests with recombinant scFv antibody fragments, wherever the notation 'Molt-4-CD19' or 'Molt-4-pLNCX2-CD19' is used. The sorting effectively removed the large majority of CD19-negative cells from the population, leaving a, mostly, uniformly high-overexpressing population.

29

Figure 4. Stable overexpression of CD19: post sort
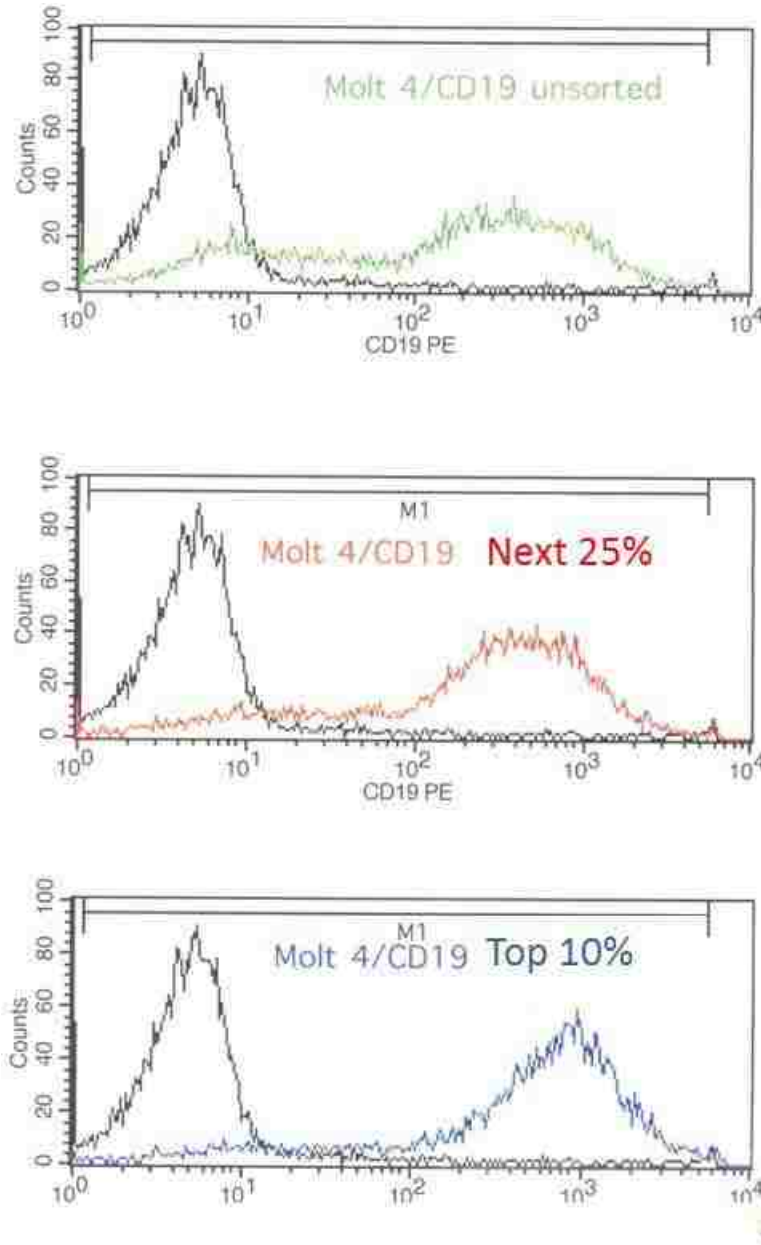
CD19 overexpression in Molt4 cells specifically increases cell death in phage panning

      Before beginning the phage panning experiments on live cells, we wanted to investigate the impact of a range of proposed panning temperatures, times and buffers to ensure that the cells were surviving the procedure. All of the four cell types that we planned to use in the panning experiments-- Molt4, Molt4-CD19, Jurkat and Jurkat-CD19-- were incubated with an aliquot of 10^{11} phage particles for either 1 or 4 hours, at either 4°C or 37°C, in PBS/0.1% BSA or RPMI/0.1% BSA. Cell viability was measured before and after the incubation (Figure 5A & 5B). Generally, high cell viability was maintained more robustly in samples incubated in RPMI/0.1%BSA at any time/temperature combination tested. Notably, the Molt4-CD19 cells exhibit a particular sensitivity to the panning procedure when incubated for four hours at 4°C (Figure 5A), but this effect can be minimized by performing the panning in simple cell culture media (RPMI) with 0.1%BSA (Figure 5B).

31

Figure 5A. Cell viability changes from different PBS/BSA incubations
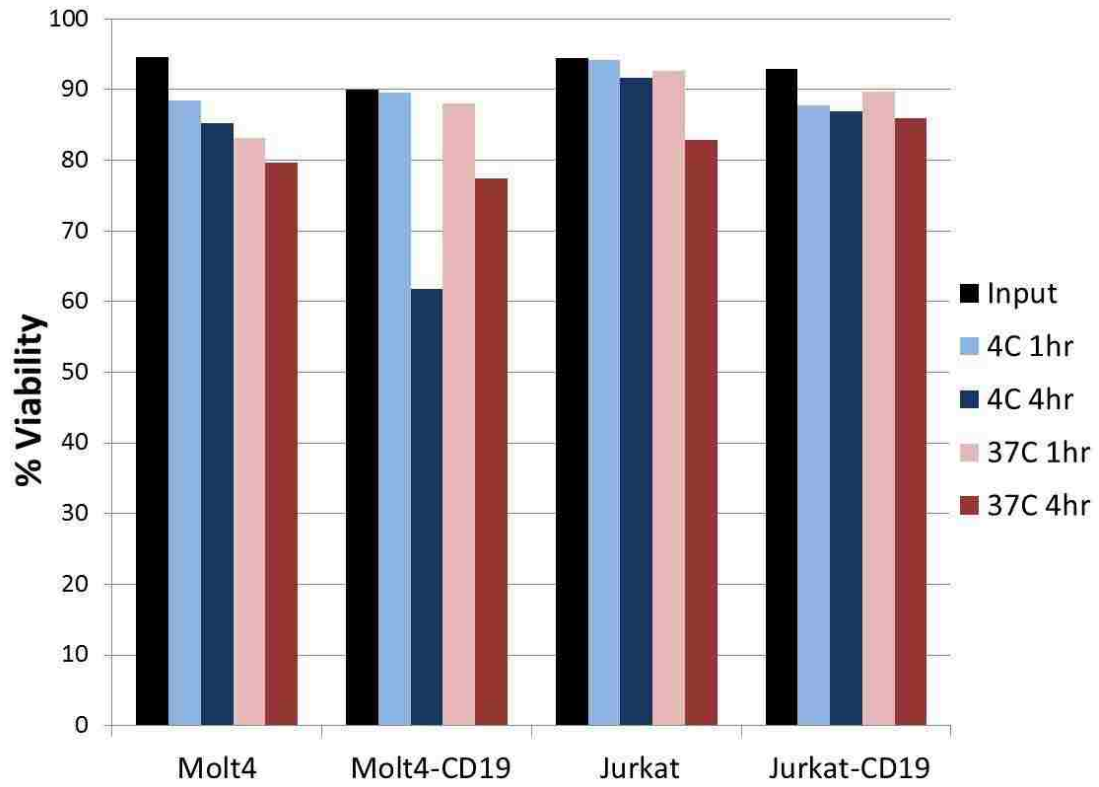
Figure 5B: Cell viability changes from different RPMI/BSA incubations
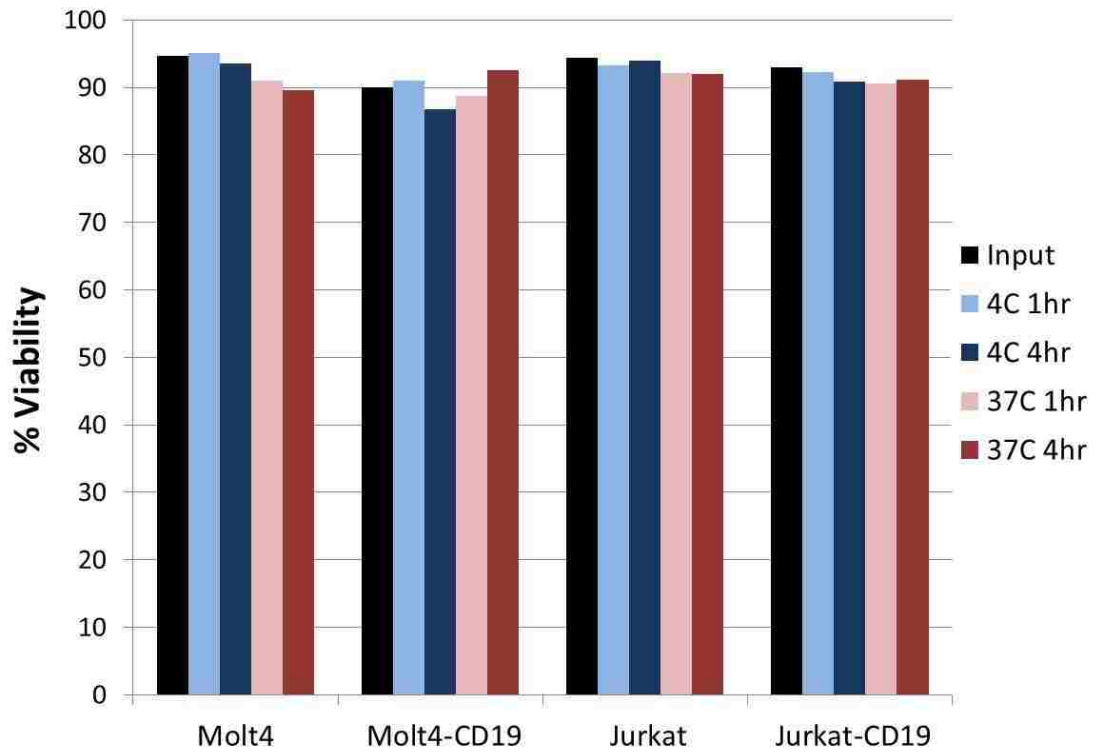
Cell-based Micropanning Assay and novel phage cleanup procedures unmask specificity of Ge11 phage

We initially had significant trouble utilizing standard assays to measure the binding of phage clones that we isolated from our screens against CD19-overexpressing cells. We wanted to develop a new cell-based variant of a screening procedure typically run in 96-well plates for testing phage clone binding to purified protein. The bound phage that are eluted are typically counted by infectious titer, which is cumbersome, has a large margin of error, and has a narrow linear range of comparison between samples. This makes the assay difficult when considering that fact that an experimenter may be screening a variety of phage clones that may have an enormous range of binding affinity from undetectable to many orders of magnitude higher.

A better option would be to use qPCR to quantify the eluted phage particles due to its relative technical simplicity and wide range. It has been previously shown that intact, infectious bacteriophage particles can be used directly for PCR without any extra DNA isolation or purification (Dias-Neto et al., 2009). The optimized protocol is described in detail in the Appendix section. Briefly, 10^{10} clonal phage particles were incubated with 100,000 cells, with triplicate samples for each CD19+ and CD19- cell lines. The samples were washed several times and the remaining bound fraction was acid-eluted and the cell debris was removed by centrifugation. The eluate was pipetted into a second 96-well plate for pH neutralization and a small aliquot was used for measurement of phage particle number by qPCR.

34

We first sought to test the linear range of the ability to use qPCR with SYBR Green as the reporter. Adding phage particles directly to the PCR reaction, we were able to plot a reliable standard curve over six orders of magnitude (Figure 6).

35

Figure 6: Direct qPCR of Ge11 phage particles

Ge11 Phage Particle Standard Curve

$y = -3.1493x + 43.772$
$R^2 = 0.996$
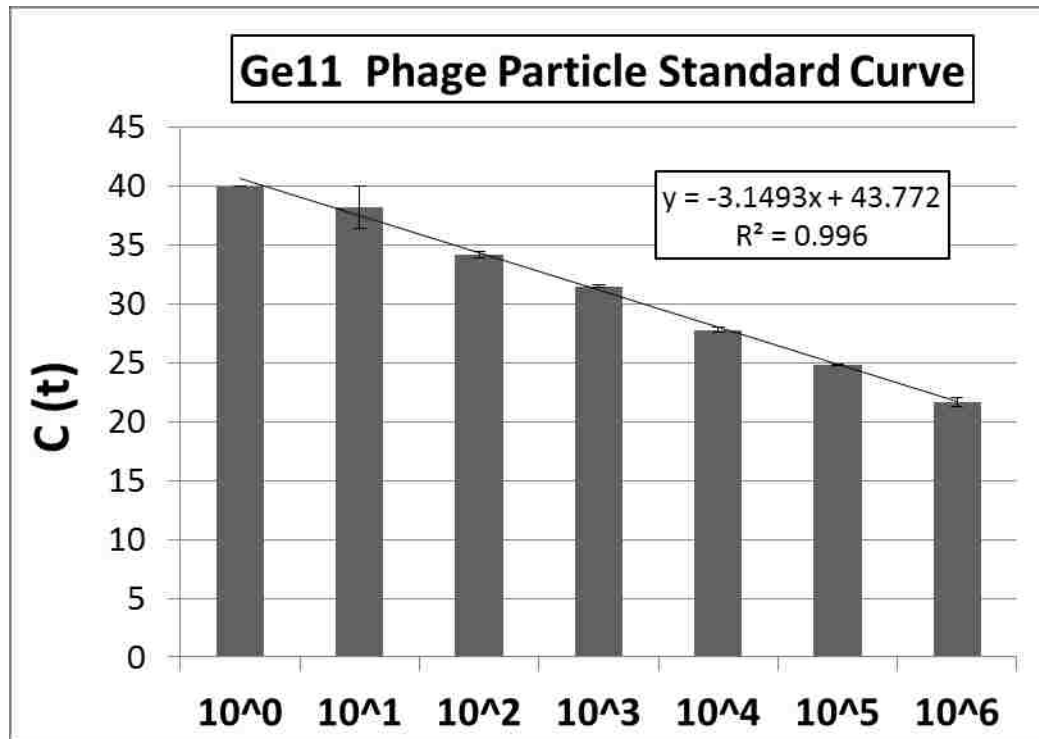
This provided a reliable way to compare phage binding to CD19+ and CD19- cells lines to test their specificity. While this standard curve varies somewhat from assay to assay in terms of absolute C(t) range (possibly due to inherent error in infectious titer plating), the slope and R^2 values remain quite reliable and serve as an excellent single-assay-based, built-in quantification control that can be run with each assay.

The next potential concern for the development of the Cell-based Micropanning Assay was whether the presence of small amounts of either cellular debris or of bacteria from the standard, incompletely purified, phage preps would significantly inhibit or cause a false positive signal in the PCR reaction. Figure 7 shows the complete obliteration of the reliability of the standard curve with the addition of small numbers of cells and that cellular DNA contributes somewhat to the signal as background.

37

Figure 7: Addition of 'contaminants' to qPCR reactions with phage
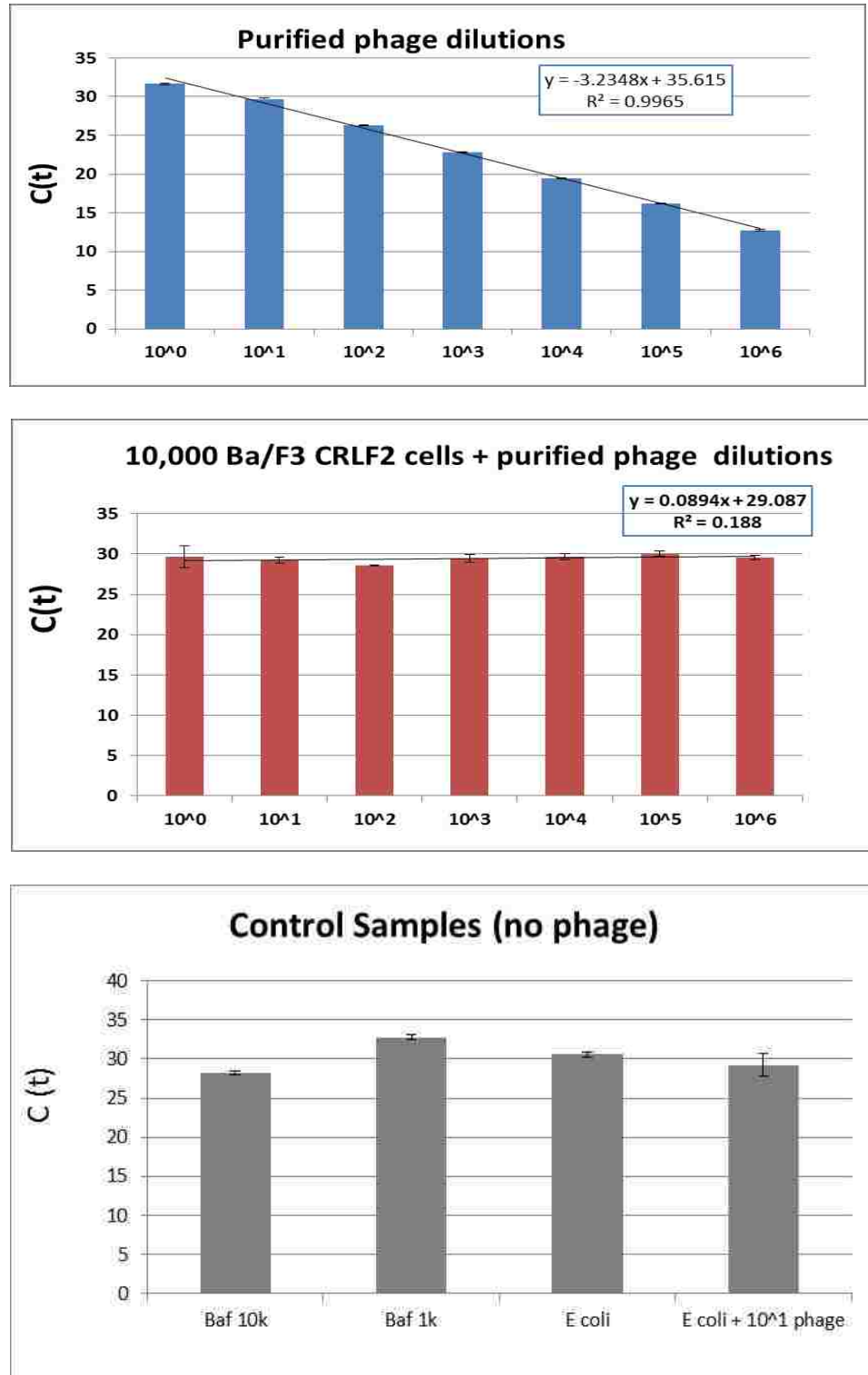
For a positive control, we used a known phage termed Ge11 that was previously isolated from the NEB 12-mer phage library with the amino acid sequence YHWYGYTPQNVI that binds with high affinity to the human epidermal growth factor receptor or EGFR (Li et al., 2005). Our lab used the mouse B-cell line Ba/F3 to overexpress human EGFR. Initially, using unpurified Ge11 phage stock directly from bacterial culture supernatant, there was no specificity of binding to the EGFR overexpressing cells (Figure 8). Also, there was very little phage recovered at all bound to cells, considering the very large input of 10^{10} infectious particles and this equivalent background binding had a dose-dependent effect, which was evidence toward the fact that the final phage recovered and used as the input for the PCR were sufficiently purified from any bacteria remaining in the phage stocks and from any noticeable amount of cell debris, when considering the dramatic effects seen above in Figure 7 (cells plus phage dilutions obliterates standard curve PCR).

39

Figure 8: Phage recovered from Cell-based Micropanning Assay: unpurified phage from bacterial culture supernatants
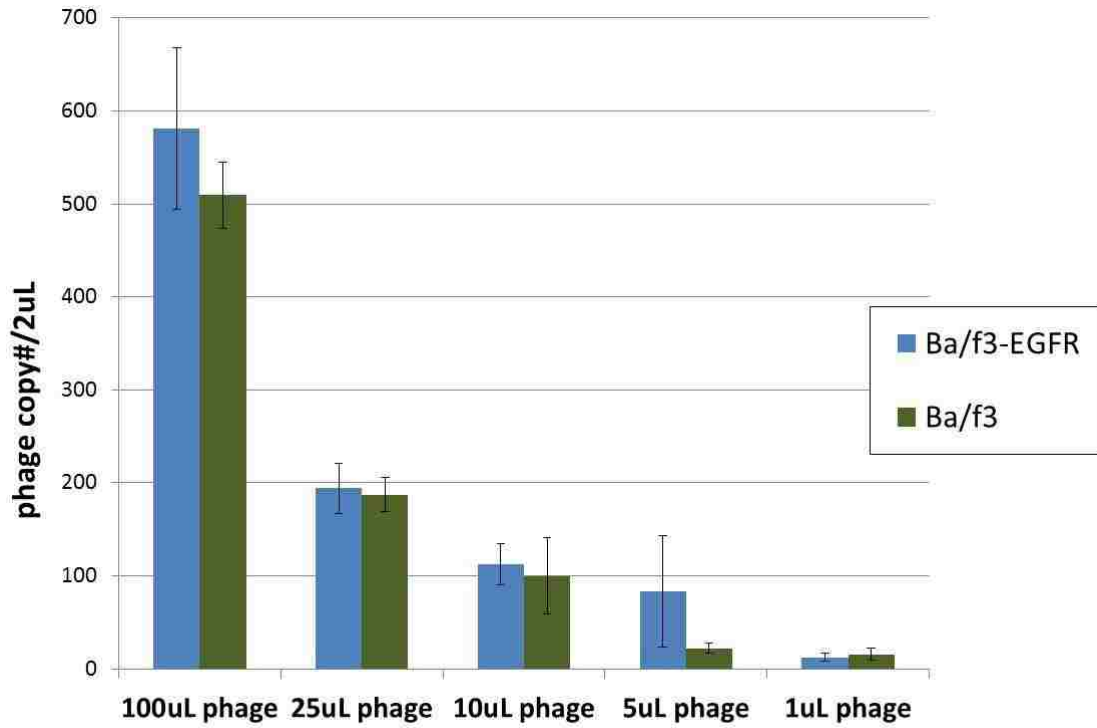
With this result in mind and the sequence of our Ge11 phage verified, we considered the possibility that impurities adsorbed to the phage surface might be inhibiting the interaction of the Ge11 peptide fused to the PIII protein on the phage with EGFR on the surface of the Ba/F3-EGFR cells. An assortment of phage cleanup procedures was tested for their efficacy to unmask the known binding specificity of this peptide. Procedures are detailed in the Methods section. One, two, and three PEG/NaCl precipitations were done, and with some samples, a variety of detergent/chemical cleanups were tried before the final PEG/NaCl precipitation (to remove the majority of the detergent) including acetic acid, CHAPS, Triton X-100, Tween, and Triton X-114-- a lower average molecular weight Triton X variant that possesses unique properties: It is readily soluble in water at 4°C but it undergoes a phase separation at higher temperatures i.e., 37°C. It is commonly used to remove lipopolysaccharide (endotoxin) from bacterially expressed protein samples (Aida and Pabst, 1990). We particularly wanted to pursue this method because *E. coli* are known to release lipopolysaccharide into the culture medium upon infection with filamentous phage (Roy and Mitra, 1970). We repeated the Cell-based Micropanning Assay using each of these differentially purified phage preparations and we found that the procedure that yielded the best binding to the EGFR-positive cells with the lowest amount of background binding was two PEG/NaCl precipitations, followed by the Triton X-114 cleanup and a final PEG/NaCl precipitation (Figure 9).

41

Figure 9: Ge11 phage Cell-based Micropanning Assay comparing phage purification efficacy for preferential binding to Ba/F3-EGFR cells
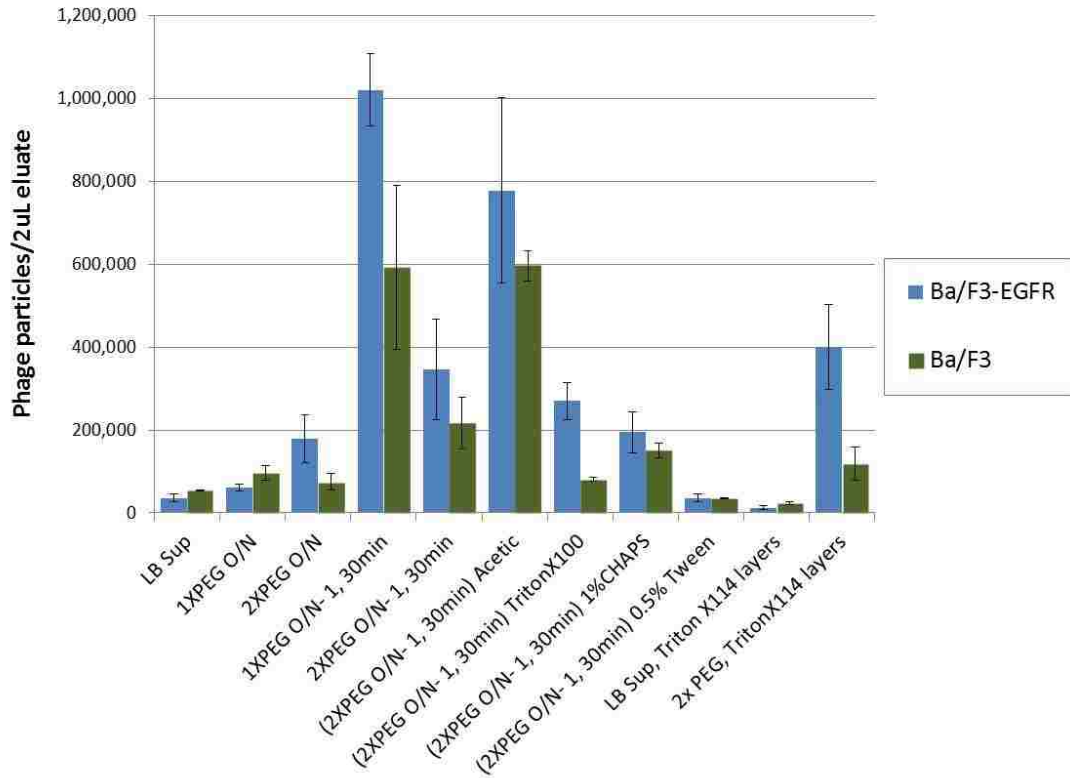
The phage cleanup procedures were further refined by adjustments of the volumes and lengthening of all the PEG/NaCl precipitations to overnight steps. This yielded particularly well-purified phage stocks that showed remarkable differential binding in our EGFR control system Cell-based Micropanning Assay (Figure 10). The fully optimized protocol is detailed in the Appendix .

43

Figure 10: Cell-based Micropanning Assay with phage purified by the optimized Triton X-114 method
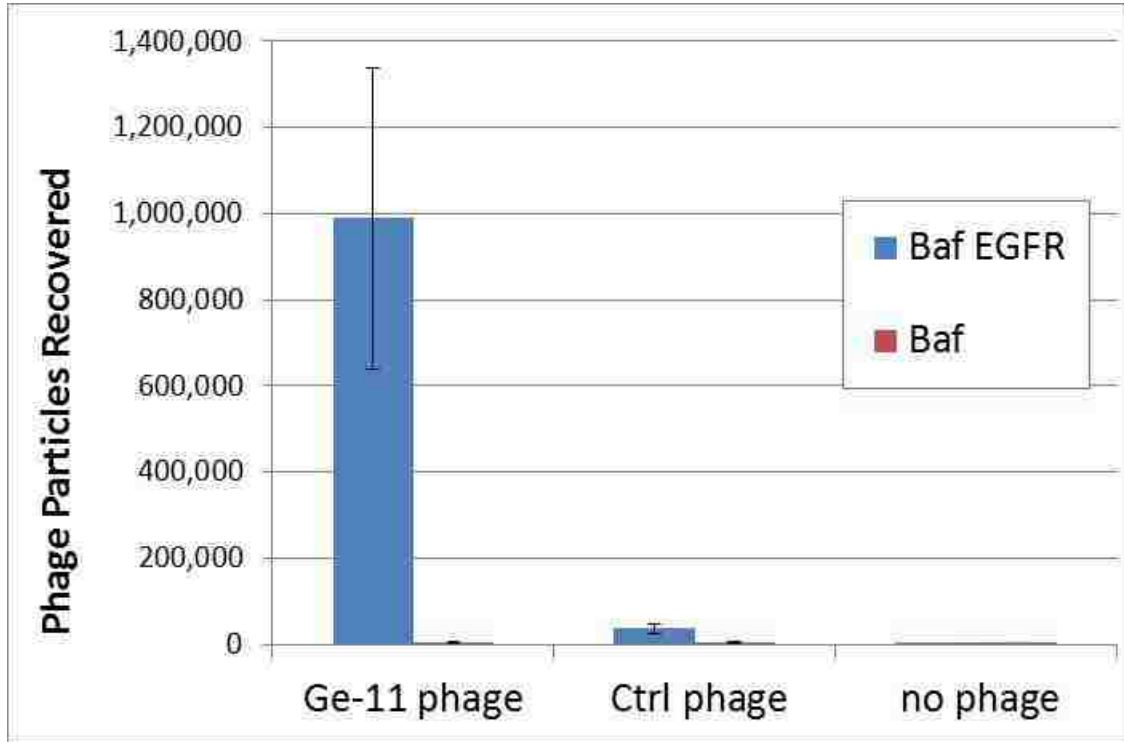
Flow cytometry for the detection of cell-bound phage particles

      With the careful optimization of the Cell-based Micropanning Assay complete, a second avenue of investigation to corroborate positive and negative results was needed. For this we turned to a flow cytometry-based approach. The micropanning assay is quite an indirect measurement, though it has many built in controls that allowed us to assume a reasonable level of confidence in results obtained therein. Flow cytometry could be done by two different methods, either by labeling the phage particle directly with a fluorophore (Jaye et al., 2004), or by doing a secondary incubation with cell-associated phage with a fluorescently tagged antibody against the phage major coat protein, PVIII. We were only able to find a single company that supplies a FITC-conjugated anti-PVIII antibody (Fitzgerald), and this antibody exhibited a high specificity toward the phage particles with minimal background on the Ba/F3 cell lines (Figure 11).

45

Figure 11: Flow cytometry measurement of Ge11 phage binding to Ba/F3 and Ba/F3

EGFR cells: detection with FITC-PVIII antibody
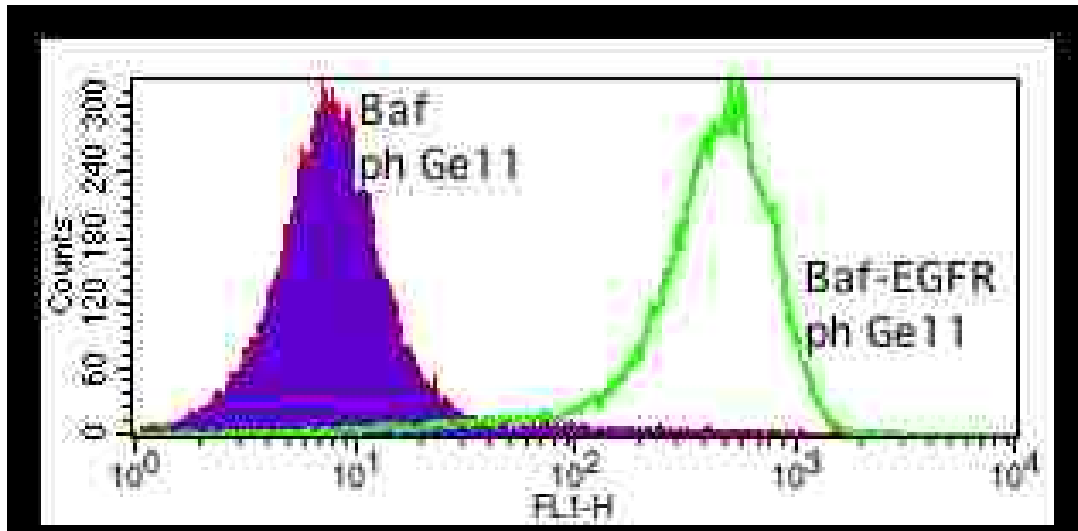
Analysis of potential CD19-binding phage clones from library screens

  With these systems in place for the analysis of clones recovered from the library
screens, we performed four rounds of selections using the protocol outlined in the
methods section, and we sequenced ten clones from each round from each elution
strategy (Figure 12A and 12B). CD77 is a molecule with two lipid chains that anchor it to
the membrane, and three sugar moieties that extend into the extracellular space and is
known to interact with CD19 in *cis* (Maloney and Lingwood, 1994). Importantly, a
chemical analog is available (Sigma-Aldrich) and it readily incorporate into the
membrane when incubated with live cells, where it may have many functions including
the inhibition of HIV infection of T-cells (Harrison et al., 2010). We employed this
parallel strategy as an attempt to more specifically collect phage that were bound to
CD19, in case the negative selections employed on the CD19-negative cells were not
effective or sufficient.

Figure 12A. Phage random peptide inserts recovered from traditional Acid elution. Highlighted sequences occur multiple times in the same or multiple rounds.

```
Acid elution              Round 2

RndB_CD19-Acid_01_1          SFNMTGTYDTPI 12
RndB_CD19-Acid_06_1          ALLRYDTKANYM 12
RndB_CD19-Acid_02_1          ELNMTTAVQNKW 12
RndB_CD19-Acid_09_1          AFNMASWDQMLL 12
RndB_CD19-Acid_04_1          SHSIRNPQWMRA 12
RndB_CD19-Acid_03_1          AVQSDHFLLWEY 12
RndB_CD19-Acid_07_1          AVQSDHFLLWEY 12
RndB_CD19-Acid_10_1          AMNMMSYMSPEP 12
RndB_CD19-Acid_08_1          HPSQEGMNDPRN 12
RndB_CD19-Acid_05_1          FRSAEXGYNMNS 12


                          Round 3

RndC_CD19-Acid_12_1          KDASRWTLQAGL 12
RndC_CD19-Acid_16_1          KDASRWTLQAGL 12
CD19R_C_Acid_17redo__1       KDASRWTLQAGL 12
RndC_CD19-Acid_15_1          GTTTLNHNYSAK 12
RndC_CD19-Acid_13_1          NRLPDWNANSNW 12
CD19R_C_Acid_14redo__1       AMNMMSYMSPEP 12
CD19R_C_Acid_20redo__1       DLPPTRRSLPLL 12
RndC_CD19-Acid_11_1          AVQSDHFLLWEY 12
RndC_CD19-Acid_18_1          SIFSIYKMMLSG 12


                          Round 4

CD19R_D_Acid_24__1           DLPPTRRSLPLL 12
CD19R_D_Acid_27__1           DLPPTRRSLPLL 12
CD19R_D_Acid_28__1           DLPPTRRSLPLL 12
CD19R_D_Acid_30__1           DLPPTRRSLPLL 12
CD19R_D_Acid_26__1           VPRLPDIWALEA 12
CD19R_D_Acid_29__1           VPRLPDIWALEA 12
CD19R_D_Acid_22__1           HKDVPKLYFHKA 12
CD19R_D_Acid_25__1           KDASRWTLQAGL 12
CD19R_D_Acid_21__1           LNRTIIPHTTSM 12
CD19R_D_Acid_23__1           HYHPLNVQLNTS 12
```

48

Figure 12B. Phage random peptide inserts recovered from Gb3 (CD77 analog) elution. Highlighted sequences occur multiple times in the same or multiple rounds.

```
GB3 elution              Round 2


RndB_CD19-GB_03_1        LANPNTRLFMKT 12
RndB_CD19-GB_05_1        SASPNVESFSHI 12
RndB_CD19-GB_09_1        STLNYHTYTVIP 12
RndB_CD19-GB_02_1        NYKVYNDRPLIR 12
RndB_CD19-GB_04_1        AMSTWAVYPGVT 12
RndB_CD19-GB_01_1        FTGSPQVLFTRP 12
RndB_CD19-GB_06_1        AVVRLYTGENLS 12
RndB_CD19-GB_07_1        SPPKQEDYGMIP 12
RndB_CD19-GB_10_1        QTNMNSTIEVQY 12


                         Round 3


RndC_CD19-GB_12_1        NDNIPKIQPIGW 12
RndC_CD19-GB_18_1        LLXRVHDPWKVP 12
RndC_CD19-GB_20_1        IPIPGERFPYSG 12
RndC_CD19-GB_11_1        GLGSMRIHWSNP 12
RndC_CD19-GB_15_1        SYDMRDTQMWKV 12
RndC_CD19-GB_17_1        SVSNGSLTRPVH 12
CD19R_C_Gb_13redo__1     LPGRAHDPWKVP 12
CD19R_C_Gb_14redo__1     TTLTYTQWRPYQ 12
CD19R_C_Gb_16redo__1     STLNYHTYTVIP 12
CD19R_c_Gb_19redo__1     DLPPTRRSLPLL 12


                         Round 4


CD19R_D_Gb_28__1         DLPPTRRSLPLL 12
CD19R_D_Gb_29__1         DLPPTRRSLPLL 12
CD19R_D_Gb_27__1         DLPPTRRSLPLL 12
CD19R_D_Gb_26__1         DLPPTRRSLPLL 12
CD19R_D_Gb_25__1         DLPPTRRSLPLL 12
CD19R_D_Gb_23__1         DLPPTRRSLPLL 12
CD19R_D_Gb_21__1         DLPPTRRSLPLL 12
CD19R_D_Gb_22__1         LPGRAHDPWKVP 12
CD19R_D_Gb_24__1         SNFNLPSKGPDE 12
CD19R_D_Gb_30__1         STLNYHTYTVIP 12
```

49

Both of the selections were stopped after Round 4 as they appeared to be converging on a single sequence, highlighted in yellow with green text above. Whether this was a sign that this particular clone displayed a strong affinity for CD19 or was simply a spurious outgrowth was not possible to tell without further testing. However, we titered the eluates from each of the first three rounds and found a steady enrichment of phage particles recovered from the FSL-Gb3 enrichment, though the acid elution strategy seemed to peak at Round 2 (Figure 13).

50

Figure 13: Progressive enrichment of phage eluates through three rounds of selection on CD19+/- cell lines: agar titer plate counts of panning eluates
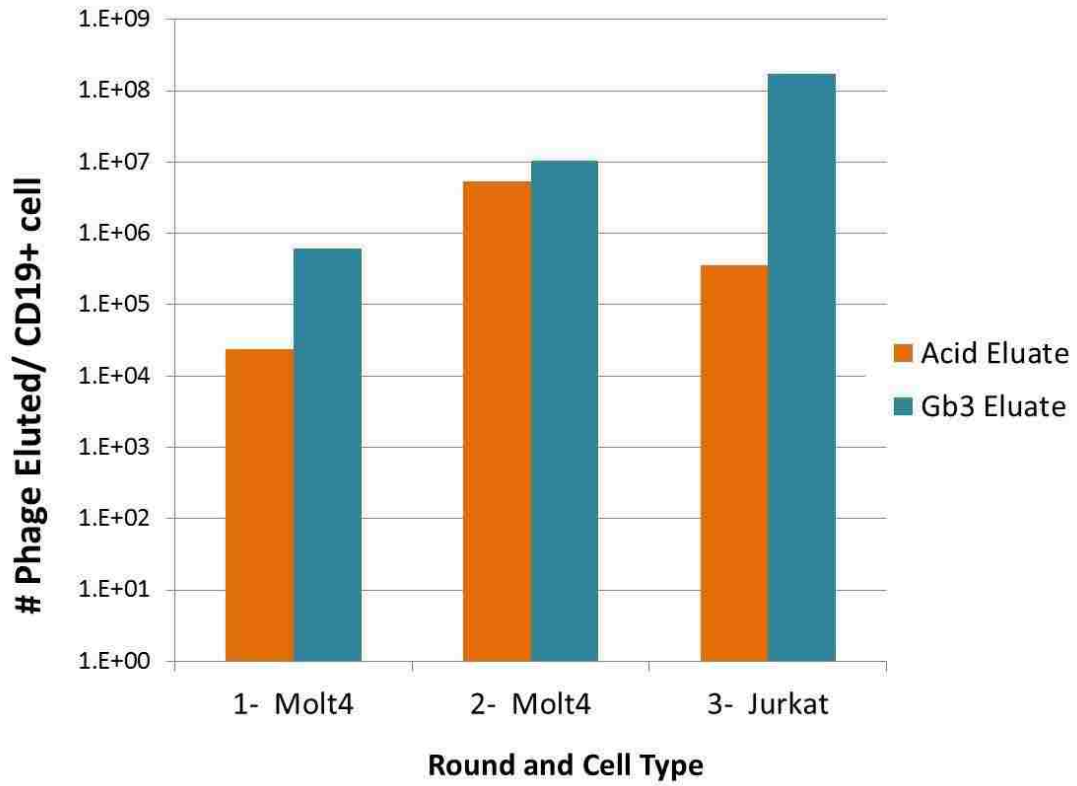
This result is suggestive that the selections were productive, though they do not rule out a number of possibilities, and certainly do not provide any specific evidence that any of the clones in these pools interact with CD19. We next began purifying these phage clones from 50mL bacterial cultures in the week-long process described in detail in the Appendix. Ge11 phage and a control phage lacking an insert were purified in tandem, with the potential CD19 clones, as controls.

Cell-based Micropanning Assay with phage clones derived from selections on CD19+/-cells

We performed the Cell-based Micropanning experiment, continuing to use the Ba/F3 and Ba/F3-EGFR cells as built-in controls with the Ge11 phage, in order to compare the binding of different phage clones to the CD19+ cells versus CD19- cells. There was significantly higher background binding of phage to the Ba/F3 cells than to the Molt4 cells, but that does not seem to limit the ability of the assay to make comparisons of binding to the Molt4-CD19 cells to the Molt4 control cells. Despite several other attempts with a large variation of phage input, none of the phage collected from this selection showed any specific binding activity.

52

Figure 14: Cell-based Micropanning Assay: testing of potential CD19 binding clones
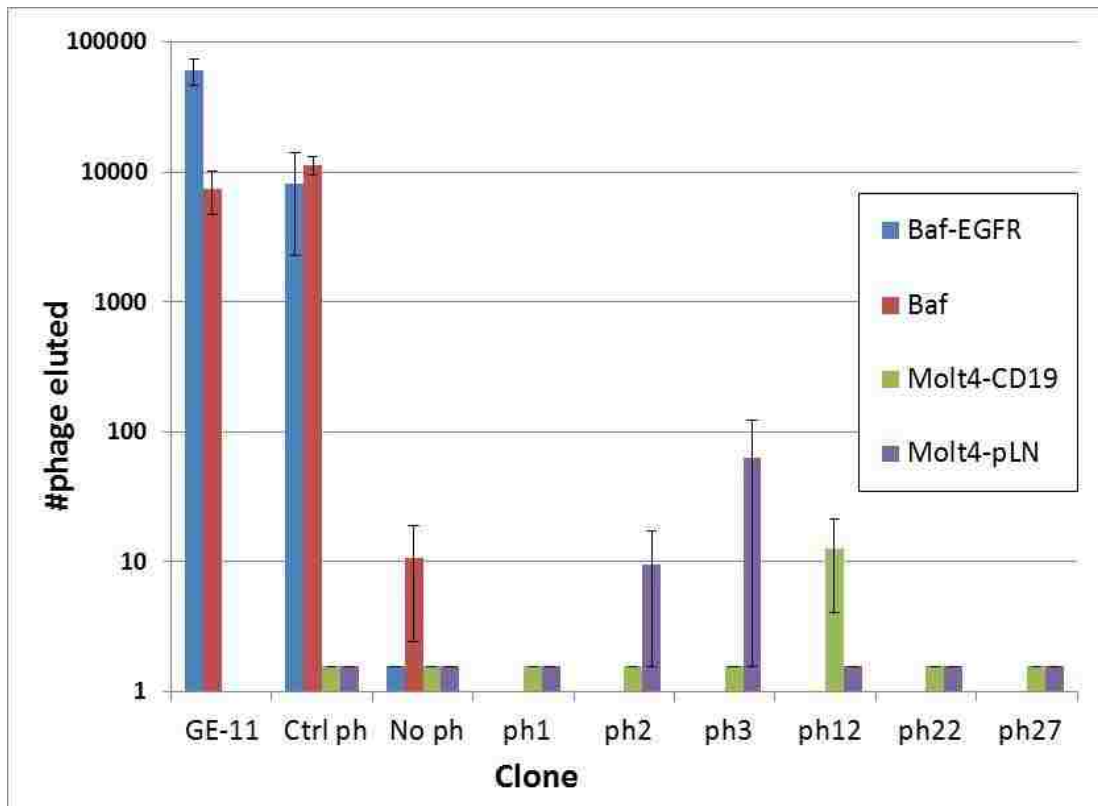
Though clone 12 here appeared to have a mild specificity, albeit on a very small scale, this result was neither repeatable nor statistically significant (P=0.324). Due to the lack of any binding of any clone tested, we wanted to validate this result, even though negative, with our flow cytometry assay.

Flow cytometry testing of potential CD19-interacting phage clones

Using the same phage stocks that were purified for the micropanning assay, as we have found them to be stable for months when stored at -20 °C, we next subjected all of these phage clones to our flow cytometry protocol optimized from the EGFR system above. A representative sample is shown in Figure 15. Again, none of these clones appeared to have any binding specificity for CD19, despite repeated attempts and changing the amount of input phage. These results taken together satisfied us in making the conclusion that the selections did not yield any CD19 binders.

Of note, we continued on with a new set of selections, performing the technique more traditionally with purified CD19 protein, as outlined in the Methods section. However, this work is ongoing in our laboratory and none of the results are available as of the date of this thesis.

54

Figure 15. Sample flow cytometry data of potential CD19 binding clones: Filled purple line is Molt4-pLNCX2 and green open line is Molt4-CD19.

55
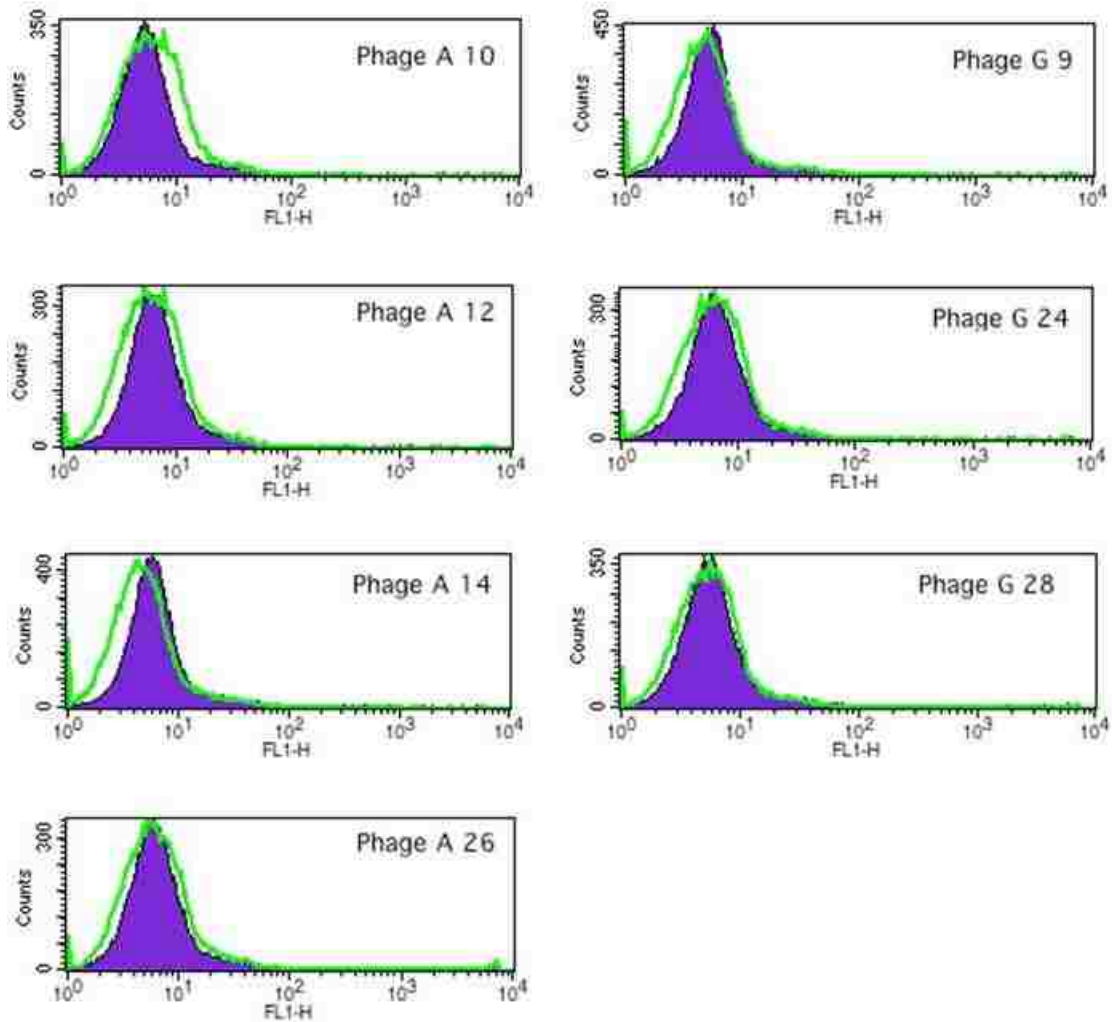
Anti-CD19 single-chain Fv fragment purification and refolding

An alternative targeting strategy to the potential, and, only theoretically possible, discovery of CD19 binding peptides from M13 phage display libraries is the production of single-chain Fv fragments recombinantly in *E. coli.* We cloned two GST-fusion protein vectors for this purpose, pGEX 6P-1-HD37 ScFv and pGEX 6P-1-FMC63 ScFv.

HD37 expression and purification

The HD37 ScFv was expressed under control of an IPTG-inducible promoter as described in detail in the Methods section. It was found to express at high levels at the expected size on SDS-PAGE followed by coomassie blue staining around 50kD. Furthermore, it appeared to be isolated almost entirely in the insoluble fraction, suggesting it was improperly folded and existed largely in inclusion bodies (Figure 16).

Figure 16: SDS-PAGE and coomasie blue staining: Expression of HD37 ScFv in an insoluble form

The inclusion bodies were then washed overnight in the detergent mixture solution outlined in the Methods section and the resulting insoluble fraction was denatured, again overnight, in 6M Guanidine HCl supplemented with 10mM beta-meracaptoethanol, 50mM Tris HCl (pH8.0), 200mM NaCl, and 2mM EDTA (pH8.0) similar to a previously published study (Umetsu et al., 2003). Some material remained insoluble after this step as well and it was discarded after centrifugation and the supernatant was adjusted to 7.5µM in the above solution after determination of the concentration by Bradford Assay. The ScFv was then subjected to dialysis with daily changes of the solution through a 3, 2, 1, 0.5, and 0M guanidine solution with addition of L-arginine and reduced glutathione at the 1M and 0.5M stages. The resulting ScFv solution remained optically clear and there was no visible insoluble pellet after centrifugation, suggesting that the ScFv now existed in a highly soluble form.

We next tested this ScFv on CD19-expressing cell lines to be able ascertain whether this soluble form had a reasonable level of specific binding activity. At this stage we took advantage of the fact that the GST portion of the fusion protein had not yet been cleaved off from the ScFv portion and we identified a fluorescently labeled anti-GST antibody that was potentially suitable for flow cytometry. Molt4-pLNCX2 or Molt4-CD19 cells were incubated with 10µL of the ScFv solution, washed and then variable amounts of secondary antibody were added from 1-20 µL. Figure 17 shows the maximum signal achieved at 20 µL of secondary antibody binding to the Molt4-CD19 cells without increasing the background binding to the Molt4-pLNCX2 cells. The upper panel shows the optimized sample overlay of the Molt4-pLNCX2 and Molt4-CD19 and the lower two

58

panels show each cell line separately with increasing amounts of secondary antibody, all

having been treated first with an equal amount of HD37 ScFv.

59

Figure 17: Specific HD37 ScFv binding to Molt4-CD19 cells by flow cytometry with anti-GST secondary antibody titration

60
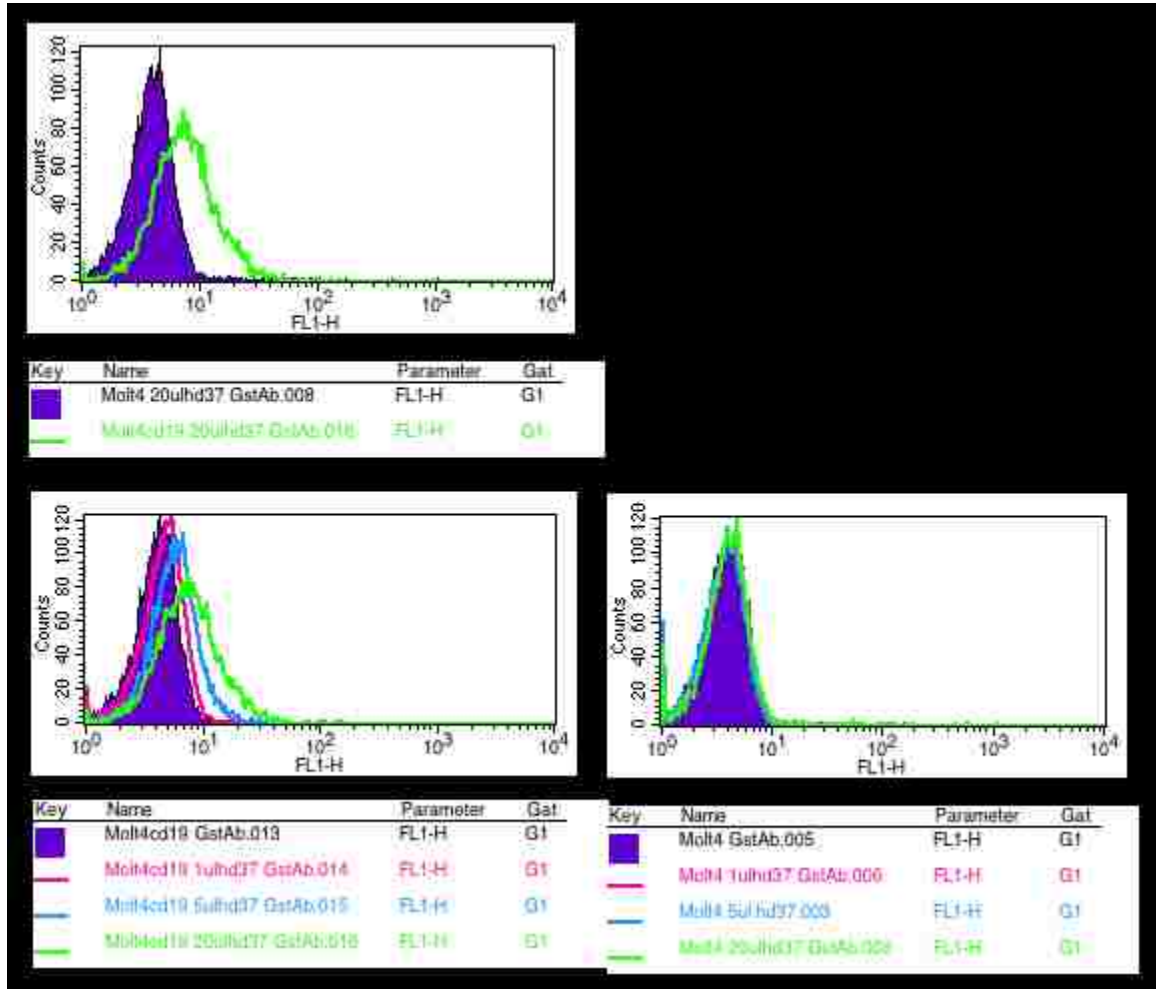
These results indicated that the HD37 ScFv was present in an active form. Though the activity was not extremely high, it was specific and acceptable from this crude unpurified extract, especially when considering that ScFvs typically have quite reduced affinities when compared to the full sized monoclonal antibodies they are derived from.

The possibility is always present that the ectopically expressed CD19 on our Molt4 cell lines is mildly different in some way from an organically expressed CD19 molecule, perhaps by differential processing of sugar modifications, minor folding differences or by being involved in or the lack of being involved in different protein complexes in these T-ALL cells versus normal B cells or malignant B cell lines. So, we tested the unpurified HD37 ScFv for its ability to bind to other CD19-positive cell lines—the pre-B-ALL lines Reh and Nalm6; we also repeated the use of the Molt4-pLNCX2 and Molt4-CD19. Having optimized the secondary antibody conditions, we also greatly increased the maximum amount of HD37 added for the primary incubation from 50μL to 250μL. Binding activity was only seen in CD19-positive cells, and was, importantly, seen in all of them (Figure 18). The binding activity did not increase dramatically and reached a maximum at the 50μL dose, perhaps indicating that bacterial contaminants remaining in the antibody solution were harmful to the cells or inhibited the binding of the antibody above this concentration.

61

Figure 18: HD37 ScFv binding to a panel of cell lines with FITC-anti-GST secondary antibody and detection by flow cytometry

FMC63 expression and purification

This particular antibody was explored in parallel to the HD37. In particular, is has the potential downstream application advantage of already being clinically approved for use against B-cell malignancies in clinical trials involving its use in gene therapy vectors used to target the patient's own T-cells against leukemia cells. We followed a very similar approach for the expression and purification of this antibody fragment as that outline above for the HD37.

The FMC 63 ScFv expression yielded a pellet that was about half the mass of the bacterial pellet from an equivalently grown culture from the HD37-bearing strain. The volumes for subsequent steps were adjusted accordingly, but the GST-FMC 63 protein was still quite insoluble and likely improperly folded. However, after the dialysis into 0M Guanidine HCl (simple TBS) the protein crashed out of solution in an insoluble form that was not solubilized by incubation at 37°C or mixing. Further, when subjected to centrifugation, Bradford Assay revealed minimal amounts of protein were left in the supernatant fraction in soluble form (data not shown). The FMC 63 ScFv is substantially different in amino acid sequence from the HD37, and though we were able to use a protocol derived from an entirely different ScFv (against hen-egg lysozyme), a different type of refolding procedure may be necessary in order to purify large quantities of properly folded, active FMC 63.

www.manaraa.com

DISCUSSION

Phage Display

At the time of this publication, attempts are still ongoing screening phage clones from the selection experiments on the purified CD19 protein. That being said, we have as yet been unsuccessful in verifying the discovery of any novel peptides isolated from the phage libraries with specific binding to CD19. While the potential explanations for this phenomena are numerous and speculative at best, a small collection of freely searchable online meta-server databases are available to explore, from a broader view, the landscape of published peptides.

Analysis of other publications

The largest and most useful of these databases (Huang et al., 2011) can be found online at: http://immunet.cn/mimodb/index.html.
The site contains information about more than 20,000 peptide sequences isolated from a large variety of phage libraries derived from over 1,000 peer-reviewed publications. The data have been sorted and categorized according to the type of library, the type of target, and importantly, the platform or 'template' that was used. While the site is by no means completely comprehensive, or free of errors plaguing the phage display literature (target unrelated peptides, etc., as discussed in the introduction extensively), some trends appear that are useful to discuss.

64

Though it was first reported almost twenty years ago that peptides against cell surface receptors (such as the urokinase receptor) could be discovered by phage display with systems very similar to ours, though with a comparatively basic procedure with only a single negative selection (Goodson et al., 1994), the literature contains remarkably few examples like this. The vast majority of peptides have, in fact, been discovered in much more reductionist biological systems, according to the MimoDB databases. By their estimation only about 2% of published peptides have been discovered using a +/- cell line overexpression system, with over 80% using purified protein and the rest targeting against various other material and chemical substrates. Due to the general dearth of published negative results in biomedical journals, two non-mutually exclusive explanations can be argued:

> 1.) The research community overwhelmingly prefers the protein-based method due to its relative simplicity compared to engineering multiple highly-overexpressing cell lines, as we did with CD19. The fact also remains that this approach has been shown to be sufficient for isolating peptides that interact with high affinity with the target, such as EGFR (Li et al., 2005), in a live cell context in downstream applications.

> 2.) The cell based approach has been tried repeatedly, yet unsuccessfully and published negative results are sparse, or commonly removed by the MimoDB algorithms for data extraction.

65

It is possible that cell-based systems, or certain types of cell-based systems, perhaps the T-ALL cell lines that we used have properties that make them unsuitable for use with phage libraries. Furthermore, it could be that most cell membrane receptors are not amenable to targeting by this approach regardless of the cell lines used, and that the small collection of strikingly important results seen in the literature are spurious, fortunate, or that certain parameters of target selection must be considered such as the specific tendencies of the receptor to be localized onto membrane subdomains with greater or lesser external accessibility to the tip of the large 900nm filamentous phage particle, when compared to relatively minute biological molecules such as antibodies. This would have to be determined on a case-by-case basis.

A final consideration is also necessary. Perhaps the assumption that any library in particular that contains at least 10^{10} unique peptides displayed should contain potential ligands against any or all proteins, such as CD19, is invalid. The library may simply not contain any phage that can successfully interact with accessible sites on CD19 (and potentially other membrane proteins). This could be due to the seemingly large library diversity still being insufficient, as the NEB Phd 12-mer library contains only about one/one billionth of all possible peptides. The 7-mer library, on the other hand theoretically contains almost all of the possible 7-amino acid peptides. Indeed most libraries of this type display peptides between 5- and 15- amino acids in length, striking a balance between low-specificity of too-small peptides, and low probability of interaction with the target/ low representation of all possible sequences of too-large peptides. It is also possible that the targetable moieties on CD19 are more likely to be bound by a

66

peptide of a particular length other than 7- or 12-amino acids due to spatial constraints of certain potential binding pockets.

It should also be noted that M13 libraries are available (both from NEB and George Smith) that display their peptides in a constrained loop due a pair of cysteine residues that flank the peptide insert, creating a disulfide bond. We did not employ this library in any of our selections and it could be a useful additional procedure to employ for the continued search of a CD19-binding peptide. The only downside with this library is that they seem to have a higher tendency to reduce the infectivity of library phage versus wild type phage, which ultimately may limit the number of rounds of selection due to wild type phage out-competing during the expansion step between rounds (according to the PhD Library User Handbook). However, due to the constrained loop confirmation, the library can be presumed to contain a remarkably different set of epitopes compared to peptides displayed 'free-floating' off the C-terminus of the PVIII protein, as the 7-mer and 12-mer libraries we employed do.

A different type of bacteriophage random peptide library

An alternative strategy for the discovery of peptides would be to use a virus-like particle (VLP) library. These self-assembling, non-infectious bacteriophage capsid particle systems can, similarly, display small peptides on their surface in both constrained and protein-terminal display strategies (Peabody et al., 2008). Importantly, these libraries, such as those based upon the MS2 bacteriophage coat protein, form icosahedral particles

67

instead of the elongated filamentous particles of M13 phage, which could, potentially, more efficiently target certain cellular receptors such as CD19. Though the use of any library will have certain drawbacks and advantages, many of which are not known, switching library platforms completely may eliminate particular biases or hurdles that were preventing the elucidation of binding peptides from the other system.

Single-chain antibodies

The HD37 ScFv antibody fragment was the only one of the two we tested that we were able to isolate and fold into a soluble form out of bacterial inclusion bodies. Though spectroscopic methods are rapidly evolving that can allow researchers to determine specific characteristics of proteins during refolding procedures that can analyze qualities such as multiple appropriate disulfide bond formations (Umetsu et al., 2003), refolding procedures generally must still be determined empirically. A good starting point for us was to use the above referenced protocol as a guide since it was working with a somewhat similar molecule, another mouse ScFv. It is difficult to speculate on any specific reasons why the HD37 antibody fragment had fairly low activity, or why the FMC 63 antibody fragment was not foldable at all into a soluble form using the same refolding procedure.

While this procedure did allow us to isolate several milligrams of HD37 ScFv in a soluble form, the binding activity of this preparation was quite lower than expected and probably insufficient for downstream applications with conjugation to particles. This is

68

especially true when compared to a report from some time ago that isolated a nearly identical myc-tagged HD37 ScFv from an *E. coli* periplasmic expression system; with only 400ng/5x10^5 cells of *crude* periplasmic extract, they were able to detect high binding activity by flow cytometry (Kipriyanov et al., 1996), whereas we saw a peak of activity that was, relatively speaking, somewhat low with up to 50-fold more protein (20 µg) by a relatively cumbersome and expensive refolding system that takes a week and large quantities of Guanidine HCl. Importantly, the periplasmic expression system in this case allowed the authors to purify about 10mg of highly active ScFv per liter of bacterial culture, which would be more than sufficient for testing in experimental nanoparticle systems.

69

APPENDIX

Appendix Part 1. Phage Display on live cells: detailed optimized procedure

Round 1 *(positive selection only)*

Day 1

1. Count Molt-4-CD19 cells and take 10^7 cells (at least 85-90% viable).

    --Note: Two samples will be run in parallel each round, acid elution and FSL-Gb3.

2. Spin 5min, 1500 rpm , decant and resuspend in 1mL RPMI/BSA(1mg/mL) in eptube.

3. Add 10uL 12-mer phage library stock (=10^11 phage particles)

4. Incubate on neutator, 4°C cold room for four hours.

5. Spin 5 min, 1500 rpm, 4°C.

6. Remove supernatant.

7. Resuspend in 1mL RPMI/BSA(1mg/mL).

-----Repeat steps 5-7, 3X-------

8. *Transfer to new ep tube to leave behind phage bound to the tube.*

9. Spin 5 min, 1500 rpm, 4°C.

10. Remove supernatant.

11. Acid: Resuspend the cell pellet in 1mL 0.2M glycine, pH2.2, (1mg/mL BSA).

12. Incubate on rotator at room temperature for 10 minutes.

13. Spin 5min, 1500 rpm, 4°C.

14. Transfer the supernatant to a tube with 150uL 1M Tris-HCl, pH 9.1.

70

15. Store O/N at 4°C. This is the *eluate*.

11. Gb3: Thaw and sonicate one 100uL aliquot of FSL-Gb3, 60%, 10sec.

       Resuspend the cell pellet in 100uL of 1mM FSL-Gb3 in (it is in RPMI w/ <u>no</u> BSA).

12. Incubate 1hr on rotator @ 37°C.

13. Spin 5min, 1500 rpm, 4°C.

14. Transfer the supernatant with GB3-eluted phage to a new tube.

15. Store O/N at 4°C. This is the *eluate*.

Day 2- Expansion of eluted phage

1. Begin a 25mL culture (phage LB + 20ug/mL Tet (1:1000) of ER 2738 from a colony < 1 week old.

2. Shake @ 37°C for ~90 min until OD600~ .01-.05.

3. Add most of the Round 1 eluate to the culture. Save ~25uL of the eluate for titering after expansion.

4. Shake @ 37°C for 4.5-5 hours (no longer).

5. Spin the culture @ 4800 rpm, 4°C, 15 min.

6. Transfer supernatant to a new tube and re-spin to pellet more bacteria.

7. Transfer upper 18mL of supernatant to a tube with 3mL 20%PEG/2.5M NaCl.

8. Mix well by 100 inversions and precipitate phage out of solution at 4°C, O/N.

Day 3 -------Continue the purification as in the NEB handbook.

1. When finished with the second PEG/NaCl purification, you should have 200uL of phage.

2. Add 700uL cold PBS.

3. Add 100uL of cold 10% Triton-X-114. Mix well.

4. Incubate on ice 30 min (Warm the microcentrifuge to 37 °C during this time).

5. Incubate at 37 °C five min. The solution will become cloudy.

6. Spin in the warmed centrifuge for 1 min, max speed.

7. The solution will become clear again and a small detergent phase (containing impurities such as LPS) will be visible at the bottom.

8. Carefully pipette off the phage-containing supernatant.

9. Bring up to ~1mL with PBS and add 165uL PEG/NaCl.

10. Precipitate at 4°C O/N and complete the next day exactly as the second PEG precipitation.

Day 4--------Titer both the eluate and the expansion.

Typical titer is about 100-1000/uL for eluate and

10^9- 10^10/uL for the expanded stock.

Round 2 *(positive and negative selection)*

Day 1

1. Count Molt-4-pLNCX2 cells and (Molt-4 CD19 cells *for later*) and take

   10^7 Molt-4- pLNCX2 cells (at least 85-90% viable).

2. Spin 5min, 1500 rpm , decant and resuspend in 1mL RPMI/BSA(1mg/mL) in ep tube.

3. Add 10^11 phage particles from the amplified Round 1 stock.

4. Incubate on neutator, 4°C cold room for four hours.

5. Spin 5 min, 1500 rpm, 4°C.

6. Transfer supernatant to new tube.

7. Use this supernatant to resuspend a fresh pellet of 10^7 Molt-4 CD19 cells.

8. Incubate on neutator, 4°C cold room for two hours.

9. Spin 5 min, 1500 rpm, 4°C.

10. Decant.

11. Resuspend in 1mL RPMI/BSA(1mg/mL).

-----Repeat steps 9-11, 3X-------

12. Transfer to new ep tube to leave behind phage bound to the tube.

13. Spin 5 min, 1500 rpm, 4°C.

14. Remove supernatant.

15. Acid: Resuspend the cell pellet in 1mL 0.2M glycine, pH2.2, (1mg/mL BSA).

16. Incubate on rotator at room temperature for 10 minutes.

17. Spin 5min, 1500 rpm, 4°C.

18. Transfer the supernatant to a tube with 150uL 1M Tris-HCl, pH 9.1.

----

19. Store O/N at 4°C. This is the *eluate*.

15. Gb3: Thaw and sonicate one 100uL aliquot of FSL-Gb3, 60%, 10sec.

  Resuspend the cell pellet in 100uL of 1mM FSL-Gb3 in (it is in RPMI w/ no BSA).

16. Incubate 1hr on rotator @ 37°C.

17. Spin 5min, 1500 rpm, 4°C.

18. Transfer the supernatant with GB3-eluted phage to a new tube.

19. Store O/N at 4°C. This is the *eluate*.

73

Repeat Day 2 and 3 exactly as above to amplify, purify and titer the Round 2 phage.

*Pick ten clones of the amplified Round 2 phage from a sparse titer plate and make DNA(500uL)/Glycerol -80C(500uL)/4C supernatant (1mL) and sequence. We will do this after every round here on out so we know when/if the library begins to converge to a small number of clones (may happen at Round 3-5 or not at all).

Round 3 *(positive and negative selection)*

Day 1

1. Count Jukat-pLNCX2 cells and (Jurkat CD19 cells *for later*) and take

   10^7 Jurkat- pLNCX2 cells (at least 85-90% viable).

2. Spin 5min, 1500 rpm , decant and resuspend in 1mL RPMI/BSA(1mg/mL) in ep tube.

3. Add 10^11 phage particles from the amplified Round 2 stock.

4. Incubate on neutator, 4°C cold room for four hours.

5. Spin 5 min, 1500 rpm, 4°C.

6. Transfer supernatant to new tube.

7. Use this supernatant to resuspend a fresh pellet of 5X10^6 Jurkat CD19 cells.

8. Incubate on neutator, 4°C cold room for two hours.

9. Spin 5 min, 1500 rpm, 4°C.

10. Decant.

11. Resuspend in 1mL RPMI/BSA(1mg/mL).

-----Repeat steps 9-11, 3X-------

12. *Transfer to new ep tube to leave behind phage bound to the tube.*

13. Spin 5 min, 1500 rpm, 4°C.

14. Remove supernatant.

74

15. Acid: Resuspend the cell pellet in 1mL 0.2M glycine, pH2.2, (1mg/mL BSA).

16. Incubate on rotator at room temperature for 10 minutes.

17. Spin 5min, 1500 rpm, 4°C.

18. Transfer the supernatant to a tube with 150uL 1M Tris-HCl, pH 9.1.

----

19. Store O/N at 4°C. This is the *eluate.*

15. Gb3: Thaw and sonicate one 100uL aliquot of FSL-Gb3, 60%, 10sec. Resuspend the cell pellet in 100uL of 1mM FSL-Gb3 in (it is in RPMI w/ no BSA).

16. Incubate 1hr on rotator @ 37°C.

17. Spin 5min, 1500 rpm, 4°C.

18. Transfer the supernatant with GB3-eluted phage to a new tube.

19. Store O/N at 4°C. This is the *eluate.*

Repeat Day 2 and 3 exactly as above to amplify, purify and titer the Round 3 phage.

*Pick ten clones of the amplified Round 3 phage from a sparse titer plate and make DNA(500uL)/Glycerol -80C(500uL)/4C supernatant (1mL) and sequence.

Round 4 *(positive and negative selection)*

Day 1

1. Count Molt-4-pLNCX2 cells and (Molt-4 CD19 cells *for later***) and take**

  10^7 Molt-4- pLNCX2 cells (at least 85-90% viable).

2. Spin 5min, 1500 rpm , decant and resuspend in 1mL RPMI/BSA(1mg/mL) in ep tube.

3. Add 10^{11} phage particles from the amplified Round 3 stock.

4. Incubate on neutator, 4°C cold room for four hours.

5. Spin 5 min, 1500 rpm, 4°C.

6. Transfer supernatant to new tube.

7. Use this supernatant to resuspend a fresh pellet of 2.5X10^6 Molt-4 CD19 cells.

8. Incubate on neutator, 4°C cold room for one hour.

9. Spin 5 min, 1500 rpm, 4°C.

10. Decant.

11. Resuspend in 1mL RPMI/BSA(1mg/mL).

-----Repeat steps 9-11, 3X-------

12. Transfer to new ep tube to leave behind phage bound to the tube.

13. Spin 5 min, 1500 rpm, 4°C.

14. Remove supernatant.

15. Acid: Resuspend the cell pellet in 1mL 0.2M glycine, pH2.2, (1mg/mL BSA).

16. Incubate on rotator at room temperature for 10 minutes.

17. Spin 5min, 1500 rpm, 4°C.

18. Transfer the supernatant to a tube with 150uL 1M Tris-HCl, pH 9.1.

----

19. Store O/N at 4°C. This is the *eluate*.

15. Gb3: Thaw and sonicate one 100uL aliquot of FSL-Gb3, 60%, 10sec.

Resuspend the cell pellet in 100uL of 1mM FSL-Gb3 in (it is in RPMI w/ no BSA).

16. Incubate 1hr on rotator @ 37°C.

17. Spin 5min, 1500 rpm, 4°C.

18. Transfer the supernatant with GB3-eluted phage to a new tube.

19. Store O/N at 4°C. This is the *eluate*.

Repeat Day 2 and 3 exactly as above to amplify, purify and titer the Round 4 phage.

76

Pick ten clones of the amplified Round 4 phage from a sparse titer plate and make DNA(500uL)/Glycerol -80C(500uL)/4C supernatant (1mL) and sequence.

Round 5 *(positive and negative selection)*

Day 1

1. Count Molt-4-pLNCX2 cells and (Molt-4 CD19 cells *for later*) and take

> **10^7 Molt-4- pLNCX2 cells (at least 85-90% viable).**

2. Spin 5min, 1500 rpm , decant and resuspend in 1mL RPMI/BSA(1mg/mL) in ep tube.

3. Add 10^11 phage particles from the amplified Round 3 stock.

4. Incubate on neutator, 4°C cold room for four hours.

5. Spin 5 min, 1500 rpm, 4°C.

6. Transfer supernatant to new tube.

7. Use this supernatant to resuspend 1X10^6 Molt-4 CD19 cells.

8. Incubate on neutator, 4°C cold room for one hour.

9. Spin 5 min, 1500 rpm, 4°C.

10. Decant.

11. Resuspend in 1mL RPMI/BSA(1mg/mL).

-----Repeat steps 9-11, 3X-------

12. *Transfer to new ep tube to leave behind phage bound to the tube.*

13. Spin 5 min, 1500 rpm, 4°C.

14. Remove supernatant.

15. Acid: Resuspend the cell pellet in 1mL 0.2M glycine, pH2.2, (1mg/mL BSA).

16. Incubate on rotator at room temperature for 10 minutes.

17. Spin 5min, 1500 rpm, 4°C.

77

18. Transfer the supernatant to a tube with 150uL 1M Tris-HCl, pH 9.1.

----

19. Store O/N at 4°C. This is the *eluate*.

<u>15. Gb3:</u> Thaw and sonicate one 100uL aliquot of FSL-Gb3, 60%, 10sec.

Resuspend the cell pellet in 100uL of 1mM FSL-Gb3 in (it is in RPMI w/ <u>no</u> BSA).

16. Incubate 1hr on rotator @ 37°C.

17. Spin 5min, 1500 rpm, 4°C.

18. Transfer the supernatant with GB3-eluted phage to a new tube.

19. Store O/N at 4°C. This is the *eluate*.

Repeat Day 2 and 3 exactly as above to amplify, purify and titer the Round 5 phage.

*Pick ten clones of the amplified Round 5 phage from a sparse titer plate and make DNA(500uL)/Glycerol -80C(500uL)/4C supernatant (1mL) and sequence.

Appendix Part 2. Detailed Cell-based Micropanning Assay protocol

An example of the documents used for the plate setup is shown below in

Appendix Figure 1.

1. In all used wells above, fill plate with complete media and incubate @37C O/N
2. Remove by shaking and blot drying just before adding cells.
3. Harvest cells and add 100uL to appropriate wells in above concentration in plate #1.
4. Add variable amount of phage sample / well (each are in 50% PBS/50% Glycerol) .
5. Seal with sticky foil
6. Incubate 4hrs, 4C neutator in cold room
7. Spin 5min 2000RPM
8. Remove supernatant by pipetting
9. WASH VOLUME #1: Add 150uL PBS/0.5%BSA per well. Resuspend well
10. Spin 5min 2000RPM
11. Remove supernatant by pipetting
12. Repeat steps 9-11 two more times, three wash volumes total (150 uL each).
13. Resuspend in 100uL 0.2MGlycine, pH2.2 +1mg/mL BSA
14. Incubate Room Temp, 15 min with gentle shaking
15. Spin 5min 2000RPM
16. In plate #2, add 15uL 1MTris, ph9.1 in all wells used above
17. Pipette up supernatant from plate#1 and transfer to duplicate plate (#2)
18. Mix well to neutralize pH
19. Run plate #3 on pcr machine immediately following.

79

Appendix Figure 1: Sample Micropan Plates: incubation and washes.

This is plate #1 (Round bottom, sarstedt) and #2 (polystyrene flat bottom) used for the initial incubation of phage and cells

PHAGE INPUT= 1 X 10^10 by pcr titer   CELL INPUT=10^5/well (100uL in media 1,000 cells/uL)

	1	2	3	4	5	6	7	8	9	10	11	12
A	GE-11	ctrl ph	no ph	ph acid 10	ph acid 12	ph acid 14	ph acid 26	ph Gb 9	ph Gb 22	ph Gb 28*	ctrl ph	no phage
B	GE-11	ctrl ph	no ph	ph acid 10	ph acid 12	ph acid 14	ph acid 26	ph Gb 9	ph Gb 22	ph Gb 28*	ctrl ph	no phage
C	GE-11	ctrl ph	no ph	ph acid 10	ph acid 12	ph acid 14	ph acid 26	ph Gb 9	ph Gb 22	ph Gb 28*	ctrl ph	no phage
D	GE-11	ctrl ph	no ph	ph acid 10	ph acid 12	ph acid 14	ph acid 26	ph Gb 9	ph Gb 22	ph Gb 28*	ctrl ph	no phage
E	GE-11	ctrl ph	no ph	ph acid 10	ph acid 12	ph acid 14	ph acid 26	ph Gb 9	ph Gb 22	ph Gb 28*	ctrl ph	no phage
F	GE-11	ctrl ph	no ph	ph acid 10	ph acid 12	ph acid 14	ph acid 26	ph Gb 9	ph Gb 22	ph Gb 28*	ctrl ph	no phage
G												
H												

Baf-EGFR   Molt4CD19 cells
Baf-parental   Molt4 plncx2 cells   10/22/2012

PCR plate (#3)

	1	2	3	4	5	6	7	8	9	10	11	12
A	GE-11	ctrl ph	no ph	ph acid 10	ph acid 12	ph acid 14	ph acid 26	ph Gb 9	ph Gb 22	ph Gb 28*	ctrl ph	no phage
B	GE-11	ctrl ph	no ph	ph acid 10	ph acid 12	ph acid 14	ph acid 26	ph Gb 9	ph Gb 22	ph Gb 28*	ctrl ph	no phage
C	GE-11	ctrl ph	no ph	ph acid 10	ph acid 12	ph acid 14	ph acid 26	ph Gb 9	ph Gb 22	ph Gb 28*	ctrl ph	no phage
D	GE-11	ctrl ph	no ph	ph acid 10	ph acid 12	ph acid 14	ph acid 26	ph Gb 9	ph Gb 22	ph Gb 28*	ctrl ph	no phage
E	GE-11	ctrl ph	no ph	ph acid 10	ph acid 12	ph acid 14	ph acid 26	ph Gb 9	ph Gb 22	ph Gb 28*	ctrl ph	no phage
F	GE-11	ctrl ph	no ph	ph acid 10	ph acid 12	ph acid 14	ph acid 26	ph Gb 9	ph Gb 22	ph Gb 28*	ctrl ph	no phage
G	10^6	10^5	10^4	10^3	10^2	10^1	10^0	H20				
H	10^6	10^5	10^4	10^3	10^2	10^1	10^0	H20				

Baf-EGFR   Molt4CD19 cells
Baf-parental   Brand new standard curve plate   Molt4 plncx2 cells

cross-hatched wells are a simple transfer of 2uL
from plate #2 to this, plate #3

Blue= GE11 phage standards added to this plate (2uL)

X MM-->	95		
	------	2	uL phage-containing supernatant
	9.5	0.1	uL of 100uM fwd primer (plus4)
	9.5	0.1	uL of 100uM rev primer (-96gIII)
	1187.5	12.5	uL 2X AB Sybr green mix
	978.5	10.3	uL H20

add 23 uL master mix to all wells, plus 2uL acid-stripped, neutralized phage from plate #2
or   2uL phage stock dilutions

Run

Standard Curve, 96 well plate   Change to 25uL reaction volume
Sybr Green "phage plus four"
95C 10 min

40X   95C 15 sec
60C 1 min
71C 30sec (Read at this temp)
melting curve

80

Appendix Part 3. Detailed phage purification protocol from a 50mL culture

<u>Day 1</u>

1.   250mL Flask. Add 50mL Phage LB & 50uL 1000X Tet stock. Innoculate with a fresh colony of ER2738 (less than 1 week old).

2.   Shake at 37°C to Abs @ OD_{600}= 0.01-0.05 (about 1.5 hours for this size culture, longer for scaled up culture).

3.   Add ~10^{10}-10^{11} phage from purified stock stored at 4°C.

4.   Shake at 37°C for 4.5 hours.

5. Pour culture into 50mL conical and spin in pre-chilled centrifuge (I-ming's) 4000X RPM, 4°C, 30 min.

6. Pipette off upper 42mL of supernatant (avoiding pelleted bacteria) and put into new 50mL conical.

7. Add 7mL 20%PEG/2.5M NaCl. Mix WELL by 100 inversions.

8. Incubate O/N @ 4°C.

<u>Day 2</u>

9. A phage precipitate should be visible. Spin in pre-chilled centrifuge (I-ming's) 4000X RPM, 4°C, 30 min

10. A white phage pellet should be visible. Remove supernatant by vacuum.

11. Resuspend very well in 10mL PBS. Vortex.

12. Spin in pre-chilled centrifuge (I-ming's) 4000X RPM, 4°C, 20 min. to pellet any insoluble matter/ bacteria remaining.

13. Carefully transfer supernatant to a new 50mL conical.

14. Add 1.65mL 20%PEG/2.5M NaCl. Mix WELL by 100 inversions .

15. Incubate O/N @4°C.

81

16. A phage precipitate should be visible. Spin in pre-chilled centrifuge 4000X RPM, 4°C, 20 min.

17. A white phage pellet should be visible. Remove supernatant by vacuum.

18. Resuspend very well in 9mL PBS. Vortex.

19. Spin in pre-chilled centrifuge 4000X RPM, 4°C, 20 min. to pellet any insoluble matter/ bacteria remaining.

20. Carefully transfer supernatant to a new 50mL conical. Pre-warm the centrifuge to 37°C.

21. Add 1mL cold 10% TritonX-114. Mix WELL by 100 inversions .

22. Incubate on ice 5min.

23. Incubate at 37°C 10 min.

24. Spin in pre-warmed centrifuge (37°C), 4000 RPM, 1 min.

25. Transfer supernatant CAREFULLY into a new tube (~about 7.5mL is all I could get off without disturbing the lower phase containing the TritonX-114).

26. Add 1.25mL 20%PEG/2.5M NaCl. Mix WELL by 100 inversions. Incubate O/N @4°C.

Day 4

28. A phage precipitate should be visible. Spin in pre-chilled centrifuge 4000X RPM, 4°C, 20 min.

29. A white phage pellet should be visible. Remove supernatant by vacuum.

30. Resuspend very well in 500uL PBS. Vortex.

31. Add 500uL glycerol and vortex until mixed well.

32. Store @-20°C.

IPTG/X-GAL Titer plate dilution: 10uL of a dilution of $1:10^7$-$1:10^9$.

OR Dilute samples $1:10^6$ to titer by qPCR. Use qPCR titer to calculate how much phage to add for the micropanning experiment.

82

REFERENCES

Adey, N.B., Mataragnon, A.H., Rider, J.E., Carter, J.M., and Kay, B.K. (1995). Characterization of phage that bind plastic from phage-displayed random peptide libraries. Gene *156*, 27-31.

Aida, Y., and Pabst, M.J. (1990). Removal of endotoxin from protein solutions by phase separation using Triton X-114. J Immunol Methods *132*, 191-195.

Azinovic, I., DeNardo, G.L., Lamborn, K.R., Mirick, G., Goldstein, D., Bradt, B.M., and DeNardo, S.J. (2006). Survival benefit associated with human anti-mouse antibody (HAMA) in patients with B-cell malignancies. Cancer Immunol Immunother *55*, 1451-1458.

Brammer, L.A., Bolduc, B., Kass, J.L., Felice, K.M., Noren, C.J., and Hall, M.F. (2008). A target-unrelated peptide in an M13 phage display library traced to an advantageous mutation in the gene II ribosome-binding site. Anal Biochem *373*, 88-98.

Davis, M.E., Chen, Z.G., and Shin, D.M. (2008). Nanoparticle therapeutics: an emerging treatment modality for cancer. Nat Rev Drug Discov *7*, 771-782.

Dias-Neto, E., Nunes, D.N., Giordano, R.J., Sun, J., Botz, G.H., Yang, K., Setubal, J.C., Pasqualini, R., and Arap, W. (2009). Next-generation phage display: integrating and comparing available molecular tools to enable cost-effective high-throughput analysis. PLoS One *4*, e8338.

Dintilhac, A., and Bernués, J. (2002). HMGB1 interacts with many apparently unrelated proteins by recognizing short amino acid sequences. J Biol Chem *277*, 7021-7028.

Giebel, L.B., Cass, R.T., Milligan, D.L., Young, D.C., Arze, R., and Johnson, C.R. (1995). Screening of cyclic peptide phage libraries identifies ligands that bind streptavidin with high affinities. Biochemistry *34*, 15430-15435.

Goodson, R.J., Doyle, M.V., Kaufman, S.E., and Rosenberg, S. (1994). High-affinity urokinase receptor antagonists identified with bacteriophage peptide display. Proc Natl Acad Sci U S A *91*, 7129-7133.

Gray, C.W., Brown, R.S., and Marvin, D.A. (1981). Adsorption complex of filamentous fd virus. J Mol Biol *146*, 621-627.

Hansel, T.T., Kropshofer, H., Singer, T., Mitchell, J.A., and George, A.J. (2010). The safety and side effects of monoclonal antibodies. Nat Rev Drug Discov *9*, 325-338.

Harrison, A.L., Olsson, M.L., Jones, R.B., Ramkumar, S., Sakac, D., Binnington, B., Henry, S., Lingwood, C.A., and Branch, D.R. (2010). A synthetic globotriaosylceramide analogue inhibits HIV-1 infection in vitro by two mechanisms. Glycoconj J *27*, 515-524.

Harvey, R.C., Mullighan, C.G., Wang, X., Dobbin, K.K., Davidson, G.S., Bedrick, E.J., Chen, I.M., Atlas, S.R., Kang, H., Ar, K.*, et al.* (2010). Identification of novel cluster groups in pediatric high-risk B-precursor acute lymphoblastic leukemia with gene expression profiling: correlation with genome-wide DNA copy number alterations, clinical characteristics, and outcome. Blood *116*, 4874-4884.

Hathaway, H.J., Butler, K.S., Adolphi, N.L., Lovato, D.M., Belfon, R., Fegan, D., Monson, T.C., Trujillo, J.E., Tessier, T.E., Bryant, H.C.*, et al.* (2011). Detection of breast cancer cells using targeted magnetic nanoparticles and ultra-sensitive magnetic field sensors. Breast Cancer Res *13*, R108.

83

He, X., Liu, S., and Perry, K.L. (1998). Identification of epitopes in cucumber mosaic virus using a phage-displayed random peptide library. J Gen Virol *79 (Pt 12)*, 3145-3153.

Ho, W.Z., Cherukuri, R., Ge, S.D., Cutilli, J.R., Song, L., Whitko, S., and Douglas, S.D. (1993). Centrifugal enhancement of human immunodeficiency virus type 1 infection and human cytomegalovirus gene expression in human primary monocyte/macrophages in vitro. J Leukoc Biol *53*, 208-212.

Huang, J., Ru, B., and Dai, P. (2011). Bioinformatics resources and tools for phage display. Molecules *16*, 694-709.

Ingle, G.S., Chan, P., Elliott, J.M., Chang, W.S., Koeppen, H., Stephan, J.P., and Scales, S.J. (2008). High CD21 expression inhibits internalization of anti-CD19 antibodies and cytotoxicity of an anti-CD19-drug conjugate. Br J Haematol *140*, 46-58.

Jaye, D.L., Geigerman, C.M., Fuller, R.E., Akyildiz, A., and Parkos, C.A. (2004). Direct fluorochrome labeling of phage display library clones for studying binding specificities: applications in flow cytometry and fluorescence microscopy. J Immunol Methods *295*, 119-127.

Kipriyanov, S.M., Kupriyanova, O.A., Little, M., and Moldenhauer, G. (1996). Rapid detection of recombinant antibody fragments directed against cell-surface antigens by flow cytometry. J Immunol Methods *196*, 51-62.

Lee, J.C., Hapel, A.J., and Ihle, J.N. (1982). Constitutive production of a unique lymphokine (IL 3) by the WEHI-3 cell line. J Immunol *128*, 2393-2398.

Lee, J.H., Engler, J.A., Collawn, J.F., and Moore, B.A. (2001). Receptor mediated uptake of peptides that bind the human transferrin receptor. Eur J Biochem *268*, 2004-2012.

Lee-Sherick, A.B., Linger, R.M., Gore, L., Keating, A.K., and Graham, D.K. (2010). Targeting paediatric acute lymphoblastic leukaemia: novel therapies currently in development. Br J Haematol *151*, 295-311.

Li, Z., Zhao, R., Wu, X., Sun, Y., Yao, M., Li, J., Xu, Y., and Gu, J. (2005). Identification and characterization of a novel peptide ligand of epidermal growth factor receptor for targeted delivery of therapeutics. FASEB J *19*, 1978-1985.

Maloney, M.D., and Lingwood, C.A. (1994). CD19 has a potential CD77 (globotriaosyl ceramide)-binding site with sequence similarity to verotoxin B-subunits: implications of molecular mimicry for B cell adhesion and enterohemorrhagic Escherichia coli pathogenesis. J Exp Med *180*, 191-201.

Maruta, F., Parker, A.L., Fisher, K.D., Murray, P.G., Kerr, D.J., and Seymour, L.W. (2003). Use of a phage display library to identify oligopeptides binding to the lumenal surface of polarized endothelium by ex vivo perfusion of human umbilical veins. J Drug Target *11*, 53-59.

Matsumura, Y., and Maeda, H. (1986). A new concept for macromolecular therapeutics in cancer chemotherapy: mechanism of tumoritropic accumulation of proteins and the antitumor agent smancs. Cancer Res *46*, 6387-6392.

Peabody, D.S., Manifold-Wheeler, B., Medford, A., Jordan, S.K., do Carmo Caldeira, J., and Chackerian, B. (2008). Immunogenic display of diverse peptides on virus-like particles of RNA phage MS2. J Mol Biol *380*, 252-263.

84

Pedersen, I.M., Kitada, S., Leoni, L.M., Zapata, J.M., Karras, J.G., Tsukada, N., Kipps, T.J., Choi, Y.S., Bennett, F., and Reed, J.C. (2002). Protection of CLL B cells by a follicular dendritic cell line is dependent on induction of Mcl-1. Blood *100*, 1795-1801.

Pezzutto, A., Dörken, B., Rabinovitch, P.S., Ledbetter, J.A., Moldenhauer, G., and Clark, E.A. (1987). CD19 monoclonal antibody HD37 inhibits anti-immunoglobulin-induced B cell activation and proliferation. J Immunol *138*, 2793-2799.

Pratt, D., Tzagoloff, H., and Beaudoin, J. (1969). Conditional lethal mutants of the small filamentous coliphage M13. II. Two genes for coat proteins. Virology *39*, 42-53.

Pui, C.H. (2010). Recent research advances in childhood acute lymphoblastic leukemia. J Formos Med Assoc *109*, 777-787.

Rahim, A., Coutelle, C., and Harbottle, R. (2003). High-throughput Pyrosequencing of a phage display library for the identification of enriched target-specific peptides. Biotechniques *35*, 317-320, 322, 324.

Reichert, J.M., and Dewitz, M.C. (2006). Anti-infective monoclonal antibodies: perils and promise of development. Nat Rev Drug Discov *5*, 191-195.

Reichert, J.M., Rosensweig, C.J., Faden, L.B., and Dewitz, M.C. (2005). Monoclonal antibody successes in the clinic. Nat Biotechnol *23*, 1073-1078.

Reilly, R.M., Sandhu, J., Alvarez-Diez, T.M., Gallinger, S., Kirsh, J., and Stern, H. (1995). Problems of delivery of monoclonal antibodies. Pharmaceutical and pharmacokinetic solutions. Clin Pharmacokinet *28*, 126-142.

Roy, A., and Mitra, S. (1970). Increased fragility of Escherichia coli after infection with bacteriophage M13. J Virol *6*, 333-339.

Smith, G. (2006). Propagation_1ml.doc.

Smith, G.P. (1985). Filamentous fusion phage: novel expression vectors that display cloned antigens on the virion surface. Science *228*, 1315-1317.

Smith, G.P., and Petrenko, V.A. (1997). Phage Display. Chem Rev *97*, 391-410.

Suntharalingam, G., Perry, M.R., Ward, S., Brett, S.J., Castello-Cortes, A., Brunner, M.D., and Panoskaltsis, N. (2006). Cytokine storm in a phase 1 trial of the anti-CD28 monoclonal antibody TGN1412. N Engl J Med *355*, 1018-1028.

Uckun, F.M., Jaszcz, W., Ambrus, J.L., Fauci, A.S., Gajl-Peczalska, K., Song, C.W., Wick, M.R., Myers, D.E., Waddick, K., and Ledbetter, J.A. (1988). Detailed studies on expression and function of CD19 surface determinant by using B43 monoclonal antibody and the clinical potential of anti-CD19 immunotoxins. Blood *71*, 13-29.

Uckun, F.M., Sun, L., Qazi, S., Ma, H., and Ozer, Z. (2011). Recombinant human CD19-ligand protein as a potent anti-leukaemic agent. Br J Haematol *153*, 15-23.

Umetsu, M., Tsumoto, K., Hara, M., Ashish, K., Goda, S., Adschiri, T., and Kumagai, I. (2003). How additives influence the refolding of immunoglobulin-folded proteins in a stepwise dialysis system. Spectroscopic evidence for highly efficient refolding of a single-chain Fv fragment. J Biol Chem *278*, 8979-8987.

Vodnik, M., Zager, U., Strukelj, B., and Lunder, M. (2011). Phage display: selecting straws instead of a needle from a haystack. Molecules *16*, 790-817.

Weber, P.C., Pantoliano, M.W., and Thompson, L.D. (1992). Crystal structure and ligand-binding studies of a screened peptide complexed with streptavidin. Biochemistry *31*, 9350-9354.

Yang, J.J., Cheng, C., Devidas, M., Cao, X., Fan, Y., Campana, D., Yang, W., Neale, G., Cox, N.J., Scheet, P._, et al._ (2011). Ancestry and pharmacogenomics of relapse in acute lymphoblastic leukemia. Nat Genet *43*, 237-241.